CORRELATION OF COMPRESSION MODELS TO MATERIAL PROPERTIES: EXPANDING PHARMACEUTICAL MODELING TECHNIQUES

By

SHISHIR VADODARIA

A thesis submitted to the

Graduate School – New Brunswick

Rutgers, The State University of New Jersey

In partial fulfillment of the requirement

For the degree of

Master of Science

Graduate Program in Chemical and Biochemical Engineering

Written under the direction of

Dr. Marianthi G. Ierapetritou

Dr. Ravendra Singh

And approved by

_____

_____

_____

_____

New Brunswick, New Jersey

October 2016

ABSTRACT OF THE THESIS

Correlation of Compression Models to Material Properties: Expanding Pharmaceutical Modeling Techniques

By SHISHIR VADODARIA

Thesis Director: Dr. Marianthi Ierapetritou, Dr. Ravendra Singh

Compression is the final unit operation in a pharmaceutical tablet manufacturing process scheme that produces the compact. Since compression determines some of the major critical quality attributes (CQA's) of tablets, such as hardness and disintegration time, understanding the effect of compression parameters on tablet quality is essential. The objective of this study is to develop a proof-of-concept methodology to correlate material properties to equipment and process performance using semi-empirical models, specifically compression models, and predict model coefficients. In this study, experiments involving some commonly used pharmaceutical ingredients such as lactose, microcrystalline cellulose, and acetaminophen was performed. The excipients were blended with varying levels of magnesium stearate ranging from 0.25 – 1.5% and the blends were characterized. The material properties measured for the blends were compressibility, permeability, cohesion, density, and particle size. Principal Component Analysis (PCA) was performed to understand the operating material design space. After tablet compaction, the compression data values were regressed to the unknown coefficients

of the Kawakita compression model and the Kuentz hardness equation. The parity plots, R-Squared (R^2) and RMSE values showed a good fit between experimental data and the model output obtained using the regressed coefficients. Partial Least Square (PLS) regression was performed using the regressed coefficient values to obtain a linear correlation between the regressed coefficients and the original blend material properties. The PLS model regression presented less than 10% error for most of the calibration points and a decent prediction of the model coefficients for the validation points. The results obtained indicate that correlations between material properties and semi-empirical model coefficients are feasible and it is possible to predict the response of model coefficients with decent accuracy. This work can be used as a basis to expand material property and process parameter correlations to semi-empirical models of other unit operations involved in pharmaceutical processing in the future.

DEDICATION

I would like to dedicate this work to my late uncle, Mr. Manu Vadodaria, who left for his heavenly abode during my stay here at Rutgers. He would be delighted to see my work shape into a platform for future research studies. Also, I would like to dedicate this work to my parents, Mr. Pankaj Vadodaria and Mrs. Dipti Vadodaria, and sister, Ms. Anvi Vadodaria, for their unconditional love and support with all my endeavors in life.

ACKNOWLEDGEMENT

I have received immense help and support from many people during my time here at Rutgers and would like to acknowledge their presence. First, I would like to take this opportunity to sincerely thank my advisors, Dr. Marianthi Ierapetritou and Dr. Ravendra Singh, for their guidance, constant support and encouragement through my time as a part of the research group at Rutgers. I would also like to thank the member of my thesis committee: Dr. Rohit Ramachandran. I am extremely grateful to PhD student, Sebastian Escotet, for his support and direction with my research right from the start. Heartfelt gratitude to PhD students, Sonia Razavi and Dr. Sarang Oka, and Dr. Sejal Shah for their time, inputs and expertise with the project. Special thanks to the Ierapetritou Research Group lab members for creating a favorable work environment and helping out with suggestions whenever needed. I am thankful to my friends and batchmates for their moral and emotional support during my time at Rutgers. Lastly, but most importantly, I would like to thank my parents and sister for believing in me and constantly motivating me to pursue my dreams.

TABLE OF CONTENTS

LIST OF TABLES

LIST OF FIGURES

CHAPTER 1

INTRODUCTION

1.1. Background

The pharmaceutical industry is a global economic sector with a revenue of over $1 trillion per year, growing at a steady rate of nearly 7% [1, 2]. Responsible for drug development, manufacturing and marketing of medications, the industry perseveres to address the world healthcare needs and hence, its importance cannot be undermined. With huge investments in research and development, there have been numerous technological advancements through time, that have helped eradicate diseases, find cure to new ones, and keep up with production to meet the global demand. Innovations and progress have helped increase average life expectancy at birth by about 6 years globally according to the World Health Organization (WHO) report [3].

The pharmaceutical industry is highly profitable due to the large profit margins in drug prices. The profit margin is as much as 20% for the big pharmaceutical companies, higher than the average net profit margins of most other industry sectors [4]. In fact, pharmaceuticals has been the major contributor under healthcare technology, making healthcare the most lucrative industry of 2015 [4]. However, the challenges faced by the pharmaceutical industry have been enormous. The complexity and rarity of diseases are making discovery and development of new molecular entities (NME) aimed at treating them, increasingly difficult. This, in addition to the varying physical and chemical properties of drug substances and rising expectations of “ideal” medical compounds (e.g. effective, no side effects, easily accessible) are contributing factors for the relatively steady

line observed in the number of NME approval filings in the last few years according to the FDA reports [6]. The number of NME approvals for the years, 2001 to 2010, have been constant within the range of 18 to 26 [6]. In fact, the number of new drug approvals (NDA) per billion US dollars spent on research and development (R & D) has nearly halved every 9 years since 1950 depicting a decline in pharmaceutical R & D productivity [7]. Figure 1 shows the declining trend of NDA per billion US dollars spent on R & D.

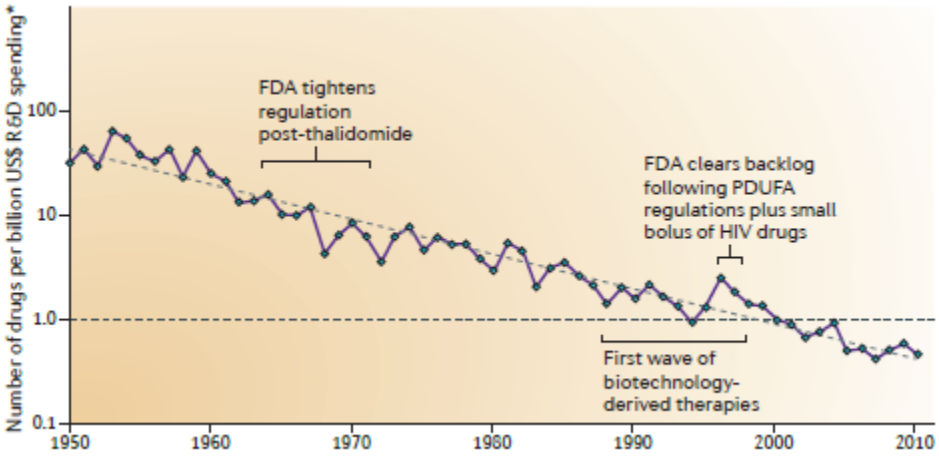

Figure 1. Trend showing a decline in the number of drugs approved per billion USD spent on R & D investment. Adapted from Scannell et al. [7].

Competition from generic manufacturers, extended drug development times, increased risk of product failures, and cost constraints set by healthcare payers have pushed companies to lower their investment cut-offs per drug molecule [5, 8]. Generics are sold at much lower prices than branded drugs, hence creating a natural preference for consumers [9]. Increased development times are affecting the period of manufacturing exclusivity earned by the companies under patent validity [10]. Since the patent system provides temporary monopoly to the issuing company, any delay in research or approval, enormously affects the profits [10]. On the other hand, the success rates for a new drug

product from Phase I to FDA approval is 32% for large molecules and only 13% for small molecules according to a study on risks associated with new drug development by DiMasi et al. [11]. With only about a quarter of drugs succeeding on an average through the clinical phase the expenditure to return ratio is relatively higher for the industry. Further, due to the availability of expertise with current procedures, continued high profit margins, and the need to get approval from regulatory agencies for any modifications in methods has made organizations reluctant to initiate changes in process schemes.

1.2. Motivation

The manufacturing scheme in the pharmaceutical industry is batch dominated and has been so from the beginning. Batch manufacturing can be described as a process that involves charging of raw materials into the system at the beginning, followed by discharge of the product after completion of the operation [12]. The complete operation is performed within the boundaries of the system, and the product is collected and stored after each unit operation before it can be transferred to the subsequent unit for further processing [12, 13]. The product obtained after each processing step is usually tested off-line for quality. If the in-process material does not meet the quality specifications for the particular step, it is either discarded, or reprocessed before moving ahead [14]. A majority of the pharmaceutical processes are poorly understood and relatively inefficient as compared to most other chemical industries [15]. Sequential scale up of batch processes, though challenging, remains the primary strategy towards process development in the pharmaceutical industry [16]. Scaling up in order to meet the market demand involves use of larger equipment, and study of material behavior and process parameters to maintain desirable product properties at that scale. This aforementioned practice, is a difficult task

due to the large number of process parameters and steps in pharmaceutical manufacturing, and does not result in the most efficient and robust production method [17]. Additionally, the steady demand of product for clinical trials, in sync with manufacturing process development, calls for expedited study of scaling up of processes [18]. The batch operation delays the processing time from days to weeks, which negatively affects productivity and profits [13]. The drug shortage issue in United States, other than the disruption of supply chain, could be attributed to the lack of agility and flexibility of the current manufacturing facilities [19]. Lack of robustness and possibility of failure could result in poor product quality consistency and hence, fewer acceptable batches [19]. The probability to introduce variation in quality from batch to batch, and a limited ability to expand production volume in the event of drug shortage or a pandemic, are some of the disadvantages of the existing manufacturing infrastructure [20, 21]. Further, the batch process method is labour intensive and requires the presence of skilled operators to function the equipment, handle materials while transporting from one step to the next and to troubleshoot.

It is the above mentioned challenges and adversities associated with the existing manufacturing practices and regulatory realities that have prompted the industry for development and implementation of newer and more reliable manufacturing technologies [21, 22]. These factors discussed above have motivated researchers, industry and regulatory bodies to collaboratively propel the industry forward through enhancement of process understanding and innovation of time and cost saving techniques [23, 24].

1.3. Technological Paradigm in Pharmaceutical Manufacturing

Continuous processing, like in other industry sectors, such as automobile, petrochemical, food and beverages, has a tremendous potential to address the economic and technical concerns of the pharmaceutical industry [17]. A continuous process is different from a batch process with respect to the amount of time the material spends in the system. Continuous process involves continuous charge and discharge of raw material and product, respectively, through the system for the period of processing [12]. As compared to batch production, continuous manufacturing helps improve efficiency by eliminating down time resulting in shorter processing times and higher throughput [20]. Additionally, continuous processing is economically favorable with lower capital and operating costs due to utilization of smaller equipment and space [17, 20, 25]. Use of smaller material volumes during processing allows for elimination of scale-up bottlenecks, especially relevant in batch method [26]. A variety of other options to increase productivity could be implemented by modification of process design, such as increasing the flowrate, using parallel processing lines or having longer run times [20]. Moreover, continuous processing decreases the amount of possibly expensive API required for process development and optimization, thus saving on material costs [20]. Flow of materials from one unit to the other reduces the amount of waste at each step leaving a smaller ecological footprint [20, 27].

Further, continuous manufacturing may aid in shortening of supply chain and making it less complicated. This would be possible because continuous processing would reduce or eliminate storage of intermediates which cannot be immediately processed under current manufacturing capabilities [20]. Continuous mode, unlike in a batch process, would

reduce the number of operators needed to be present on site since transfer of materials from one unit to the other would not be required. Lastly, it could diminish the variability in product quality through use of real time process control techniques [21, 22]. All of these benefits offered by continuous processing, in addition to its successful execution in some of the other industries named above, have made it an attractive option for pharmaceuticals as well.

However, there are numerous technical, operational, regulatory, and workforce challenges, that need to be addressed before it can be widely adapted as a manufacturing strategy [28]. Technical challenges may involve thorough understanding of process models and material attributes for development of good process control strategies, evaluation of potential failure points and coming up with optimal solutions for efficient process dynamics, such as start-up and shut-down [20, 29]. Development and operation of this new technology could demand presence of highly skilled and trained workforce, who are able to gain expertise of the process as a whole [28]. Since the pharmaceutical industry is strictly regulated, any significant modifications in process technology would require approval from the respective regulatory agencies in different countries, depending on the location of the manufacturing facility, and this could result in regulatory delays.

Bearing all of these potential challenges in mind, modernizing of pharmaceutical processes has been well recognized and supported by the FDA. Use of PAT (Process Analytical Techniques) tools to enhance QbD (Quality by Design) efforts has been encouraged [30]. A number of documents relevant to QbD approaches have been issued over time by the FDA in order to provide guidelines on its application [20]. The shift from batch to continuous manufacturing will allow for real time characterization through use of

state of the art process analytical tools and hence provide control over drug quality, thus being consistent with the belief and realization: "*quality cannot be tested into products; it should be built-in or should be by design*" [31]. These tools are extremely useful with respect to quality control (QC) and quality assurance (QA) of drug products in the pharmaceutical industry.

1.4. Application of Process Systems Engineering in Pharmaceutical Process Development

Efforts by the industry, academia and regulatory bodies have made continuous manufacturing of solid dosages a reality, but it is still a long way from being widely used for manufacturing of drug products. It is essential to achieve a thorough understanding and develop expertise of the process systems that will be implemented since these will have huge impact on product quality [32]. Process development includes planning the supply of API for toxicological and pre-formulation studies, followed by supply of drug product for clinical trials, and finally creation of an environmentally benign, economically viable and technically sound production process [33]. Evaluation of critical material properties as a function of operating parameters would be essential to analyze and optimize individual processes and hence mitigate risks associated, by identification and assessment of design elements.

Application of Process Systems Engineering (PSE) tools would be highly effective in this endeavor to facilitate a structured transition from batch to continuous manufacturing [17]. This would involve building of mechanistic models for representing process knowledge, developing algorithms and advanced process control methods with the help of computer-aided engineering tools [34]. Simulation of pharmaceutical processes, along with

flexibility analysis could be useful in identifying operating variables affecting product attributes as well as aid in process operation design and optimization [35]. Online measurement of material properties (i.e. process variables) through application of various analytical tools could help gain knowledge and collect real time data of the transformations occurring *in situ*, which could form the basis for predictive process models [36]. These models could then be utilized to develop control strategies to ensure uniform product quality.

There are a variety of PSE tools that can be applied to achieve various process development objectives. As mentioned previously, predictive models could help to improve process understanding, while feasibility and flexibility analysis could assist in setting process parameter ranges. Sensitivity analysis would be effective in risk management, dynamic optimization could be applied to improve process efficiency and steady state optimization to better product and process design. Flowsheet modeling would allow for integration and simulation of continuous operations along with implementation of control design pattern to govern the product characteristics [35].

1.5. Predictive Flowsheet Modeling

Advanced process modeling in the pharmaceutical industry has not been as developed, compared to the chemical, petrochemical, food and other industries. Computer Aided Process Design (CAPD) and other simulation tools have been widely useful in chemical and petrochemical industries since the early 1960's in expediting the process design and optimization study [33]. Modeling of solid dosage processes especially, have not yet been well established due to their discrete nature, which has resulted in limited study in the area [37]. On the other hand, all of this is changing because of the various

initiatives that have been taken by industry in collaboration with academic institutions and with support from FDA, to enhance and document their process understanding in the form of models that could help reduce the high number of experimental trials during early stages of product development and mitigate risks of failures when implemented [38]. Development of dynamic modeling software packages, such as gPROMS® and gSOLIDS®, from Process Systems Enterprise, Aspen Plus™ and Hysys® from Aspen Technology, Inc. and others, especially those applicable and specifically designed to cater pharmaceutical processes has helped immensely in creating predictive models with fair amount of accuracy [39, 40].

Models are mathematical relationships used to describe the occurrences in a system. Mathematical models could be extremely useful in pharmaceutical engineering because of their ability to provide information about the macroscopic properties of a system, using microscopic equations depicting the behavior of the materials within the system [41]. Application of models could substantially reduce the time and costs associated with experimental trials [41]. However, in order to prove the credibility of these models, it is important to validate the output from the models with experimental data [41]. Further, fine tuning and estimation of certain unknown parameters present in the model may need to be done. On completion of this step, verified and validated (V & V) models are obtained, which can be used as a process development and optimization tool [17, 41]. Models can be divided into sub-categories depending on the fundamentals of development, complexity, and the depth of information they provide that could be useful for a powder system. Some of the models that could be useful in pharmaceutical technology have been briefly explained below. A detailed review of the models that could be implemented in

development of processes for solid-based dosage forms has been provided by Rogers et al. [17].

1.5.1. First Principles Models

First principles models are based on the principles of mass, energy and momentum conservation and the fundamental laws of physics [42]. First principles models are expected to be better than statistical models, which have low tolerance and require high amount of experimental data. First principles models can be sub-divided into discrete and continuum models. Discrete Element Models (DEM) involve modeling of discrete powder particles by defining the motion and behavior of the particles in space with the help of basic physical and mechanical principles [43]. In DEM, each particle is modeled individually, and the position and velocity of particles can be used to calculate certain quantities of interest, such as concentration and particle stresses, or study particle phenomena, such as segregation and aggregation [43]. DEM is beneficial since it provides a detailed output for a system of dynamic particles and allows for a comprehensive study of the effect of material properties, process variables and equipment design on the efficiency of the system [43]. However, DEM requires substantial computational capability, may involve longer simulation times depending on the size of the system, and can be expensive [43]. On the other hand, continuum models such as Computational Fluid Dynamics (CFD) are used for continuous systems, such as liquids, gases and dense solids, where particle-particle interactions can be ignored [43]. Fundamental transport phenomena principles are applicable for continuum models. The approach used in CFD is most accurate for systems involving fluids [43]. Dilute solid systems can also be modeled via this approach. For dilute solid systems, the solids can either be assumed as a second continuous phase and the

equations solved accordingly, or modeled discretely using DEM [43]. Like DEM, CFD modeling also requires decent computational power to run software packages such as ANSYS® Fluent, efficiently.

1.5.2. Multi-dimensional Models

Multi-dimensional models, such as Population Balance Models (PBM), describe the state of particle population as a function of time, as well as predict the changes occurring within the population [44]. In particulate processes, it is necessary to incorporate particle population balances in the model, in addition to the general mass and energy balance equations to capture the compartmental (population) behavior [44]. Multi-dimensional models are typically used to model processes which involve modification in material properties (e.g. particle size, porosity, density), such as granulation, milling etc. [45, 46]. The general population balance equation stated by Randolph and Larson (1971) recognizes the characterization of particle population with the help of internal and external coordinates of particles [44]. Internal coordinates include intrinsic properties such as porosity of a particle, and external coordinates take into account exterior factors such as particle velocity, and hence capture a combined effect on the population state [44, 46]. Application of multi-dimensional models in pharmaceutical operations can aid in design, control and optimization of particulate processes to achieve desirable product attributes [44, 45]. Multi-dimensional models for continuous powder mixing and wet granulation processes have been discussed in Sen et al. and Barrasso et al., respectively [45, 46].

1.5.3. Semi-empirical Phenomenological Models

Semi-empirical models are based on theoretical first principles models with certain parameters estimated using experimental data or calculated from equations and fundamental constants [47]. Since some of the parameters are obtained with empirical data and most of the equations are based on theory, these models lie between purely empirical and purely theoretical [47]. Parameters obtained from experimental data for a specific combination of material and equipment help with model calibration [48, 49]. Calibration is done in order to maximize the agreement between experimental data and model output [49]. The complexity of the model can be reduced with the help of certain well-made assumptions.

Semi-empirical models do not provide a detailed output about the system, unlike DEM and CFD, but provide decent information about the system's behavior by relating model variables and operating conditions. These are lower dimensional models that are relatively less cost-intensive and involve shorter simulation times than DEM, PBM or CFD. A good example of these models are low dimension population balance models such as the residence time distribution (RTD) model. RTD models aid in understanding the transport of particles within a unit operation and the effective time spent by the material inside the system [50, 51]. Experimental studies for RTDs can be carried out using tracers, which are non-reactive, easy to detect elements added to the system, whose path can be traced back and the desirable variables quantified at the outlet [51]. The probability density function can be used for tracers to compute the distribution of time spent in the system [51]. A stimulus response via a pulse or step change can be performed at the inlet to study the steady state point in a continuous system and the tracer concentration can be recorded

at the outlet [50]. Application of RTD models in solid processes such as continuous blending, extrusion, with industrial advancements in the area have been reviewed by Gao et al. [50]. RTD models can aid in predicting mixing regime, system throughput, product composition and many other factors required to improve the understanding of a unit operation. Therefore, these can be effectively utilized in modeling of various pharmaceutical operations.

1.5.4. Empirical and Reduced Order Models (ROM)

Empirical and reduced order models are low dimensional models that allow for computationally inexpensive mathematical representation for real time system analysis [52]. The construction of ROMs could however be costly due to the need of accumulating system responses [52]. ROM may lack robustness with respect to parameter changes and may have to re-built for each parameter variation [52]. As opposed to any other model type previously described, these models have hardly any relationship with the system's phenomena and are merely regressions of data available for the system. Heavy dependence on data makes them ineffective in areas where there is no input available. Due to inexpensive computations, these models are useful for design of control systems and their development.

1.5.5. Flowsheet Modeling

Integration of processes involves connection of individual unit operations with piping in a series to perform a sequential completion of tasks to enable conversion of raw materials to desirable product(s) without isolation of intermediates [35]. The output of a preceding unit becomes the input of a subsequent one in this case, with material

continuously flowing between them [35]. This logic works mathematically as well. Models of individual equipment can be integrated as a flowsheet by taking the results from a preceding model and using it as the inputs of the subsequent one. These so called flowsheet models, that allow for the flow of information between the unit models resemble the flow of material(s) between unit operations [35]. Flowsheet simulation can enable process engineers to identify integration bottlenecks, if any, and hence work on the issues beforehand, point out contrasting design and control objectives, study the effect of start-up and shut-down on process efficiency, thus reducing integration efforts and down-time [53].

Modeling and simulation of processes have numerous benefits in research and development. *In silico* experimentation substantially reduces material requirement for physical experiments, and hence reduces the associated costs during early stage product development. Additionally, it expedites the drug development study, thereby shortening development times. Overall, models can help to enhance process knowledge, identify the key process variables and maintain them within a design space defined by the desired product properties [54]. Models can further assist in optimization, risk assessment and development of control strategies to ensure reproducible product quality [17]. The result is a potential robust and reliable manufacturing process that can consistently meet the stringent quality requirements mandated by regulators (e.g. FDA). Owing to the various benefits observed, modeling of pharmaceutical operations has become a desirable and pursued field.

1.6. Tablet Manufacturing Process

1.6.1. Process Overview

Solid oral dosages are the most common type of pharmaceutical drug dosage forms, mainly because of the ease of administration and storage, and their widespread acceptance among consumers [55]. Together, capsules and tablets capture more than 50% of the pharmaceutical drug market, out of which tablets account for the majority, since they are simpler to manufacture than capsules and have longer shelf life than most liquids and capsules. Due to their ubiquity in the medicinal world, extensive research is being carried out to understand and improve the existing manufacturing processes of these powder compacts to meet the desired quality standards and strict regulatory (e.g. FDA) specifications.

The contemporary tablet is a complex mixture of a number of compounds, in the present context well-known as excipients, in addition to the active drug substance (Active Pharmaceutical Ingredient (API), added to impart certain functionalities to the formulation. There are numerous reasons that make addition of extra elements rationale. First of all, most of the APIs have a limit on the consumption quantity due to toxicological and other factors, which restrict their bulk volume to extremely small volumes. Therefore, addition of excipients helps to increase the bulk volume to tangible quantities, also classified as bulking agents. Secondly, manufacturing of tablets involves the process of compression, and not all API are easily compressible and hence may require higher than practical compaction and ejection forces. Incorporation of excipients helps to modify these material properties to bring process variables within operating ranges and ensure smooth functioning of the system. Lastly, different excipients are aimed at achieving desirable

critical tablet qualities and hence dependent *in vivo* functionalities. Some of the commonly used pharmaceutical excipients can be classified into types depending on their application, as bulking agents, binders, disintegrants, coatings, lubricants etc. [56].

There are various routes of manufacturing a tablet: Direct Compaction (DC), Wet Granulation (WG) and Dry Granulation (DG). Figure 2 is a schematic representation of the unit operations involved with the different routes. The manufacturing process chosen varies depending on the raw material and formulation properties [17]. Direct compaction is the least complex and fastest way to produce tablets out of the three. But, direct compaction requires a careful selection of components in order to ensure a successful compaction operation. On the other hand, granulation processes are used to achieve the desired flow properties suitable to carry out the compression operation smoothly. Irrespective of the route followed, compression is the final unit operation as it allows us to take advantage of plastic deformation and bonding mechanisms of materials to form hard, durable compacts. Since this process governs the important tablet properties that affect the critical quality attributes (CQA's) laid down by regulators, it is critical to understand and hence optimize the process to achieve production consistency.

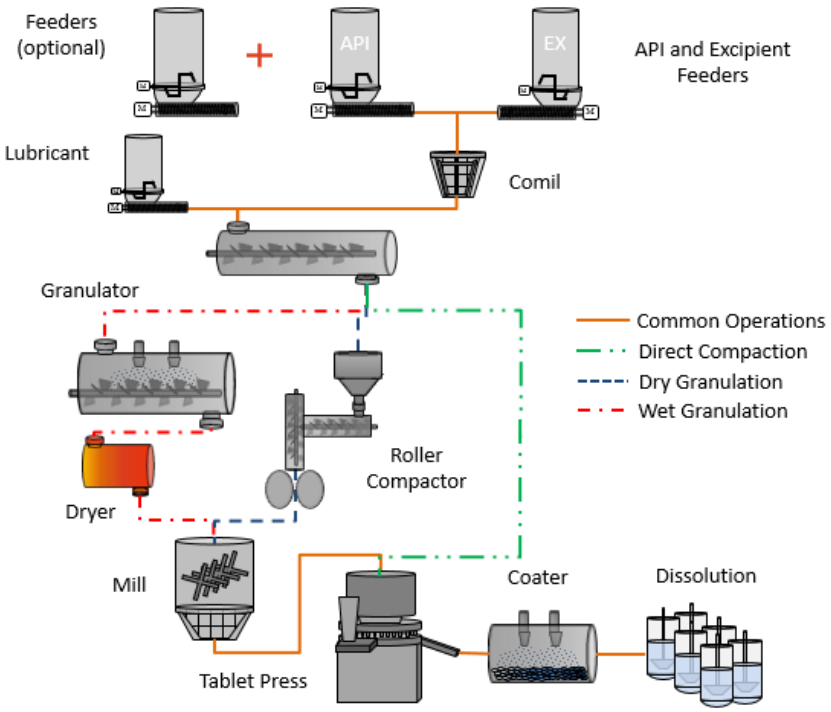

Figure 2. Flexible continuous manufacturing process [35].

The general downstream continuous manufacturing process usually starts with feeding of raw materials including the active pharmaceutical ingredient, excipients, and lubricant with the help of feeders. The feeders have an integrated hopper to hold certain amount of material and a rotating screw to vary the flow rate [57]. The comil is used to mill down lumps. The material is then blended to ensure a homogeneous mixture with a uniform distribution of the API that would help maintain the requisite API content in tablets. After the blending operation, the mixture is either directly passed on to the feed frame via the hopper attached to the tablet press for the compression process, or granulated via wet or dry granulation process. If granulation is implemented, milling is usually performed to reduce the granule size to a desired range. In case of wet granulation, drying of granules before further processing is needed [17]. Roller compaction is utilized for the

dry granulation route, especially when the formulation is known to be sensitive to moisture. Ribbons obtained from the roller compactor are milled to smaller particle sizes in the mill [57]. In order to ensure consistent particle size range, the oversize particles are recycled to the mill while the undersized particles are sent back to the roller compactor [57].

1.6.2. Tablet Press Operation

Tablet Press is the final unit operation that compresses pharmaceutical powder blends to give tablets of uniform size and weight. Since fast paced production of these miniatures is necessary to keep up with the global demand and knowing well that tablet presses govern the critical table properties, these devices are essential to the pharmaceutical industry. Tablet Press consists of several components, all sophisticatedly packed in this compact space. Hopper, feed frame, turret, punches and dies are the main parts involved with compaction operation in a rotary tablet press. The hopper holds the material to be compressed. The material is transferred from the hopper into the dies via the feed frame, which pushes the powder with the help of rotating blades on to the turret. The turret is rotatable and consists of multiple die stations, each with an upper and lower punch that can move vertically to compress the powder. Once the powder is pushed on to the turret, the lower punch moves downward allowing the powder to fall gravimetrically into the die while creating some suction during the filling stage. Following this, the upper punch and lower punch compress the powder in the die at relatively lower pressures during the pre-compression step designed to eliminate air gaps that could potentially affect tablet porosity and hence hardness. The final compact is formed during main compression when much higher pressures are applied resulting in products of desirable hardness. Subsequently, the tablet is ejected as the lower punch moves upward and the upper punch back to its initial

position. Cam tracks guide the movement of punches through these various stages of a tablet press cycle. The shape and size of the tablet is governed by the geometry of the die and punch used. Nowadays, companies can be seen making great use of this flexibility for marketing by using custom built punches that inscribe the brand name on tablets. Figure 3 below is a schematic representation of the various stages observed in a rotary tablet compression system.

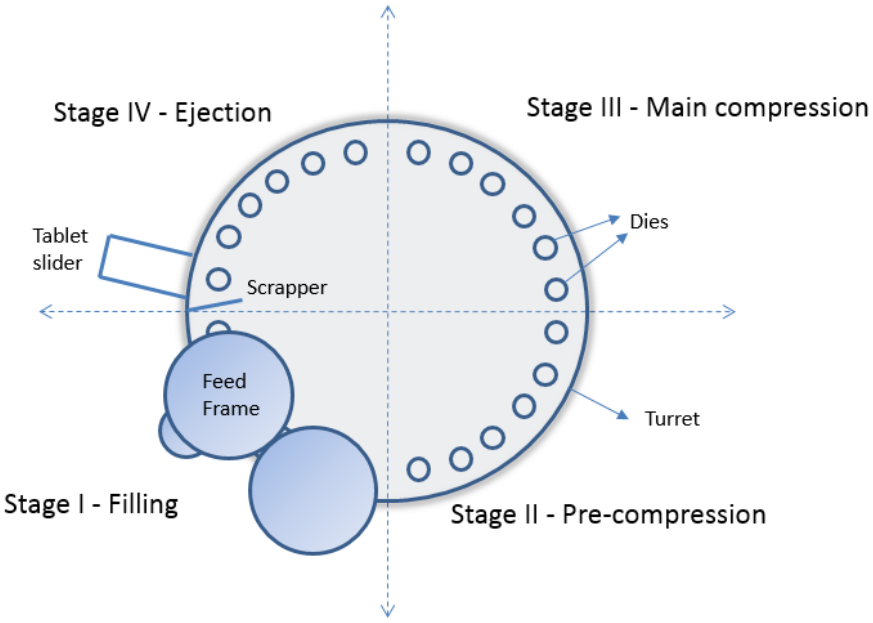

Figure 3. Schematic representation of the top-view of feed frame and turret arrangement in a rotary tablet press depicting the various stages in the tablet compression process.

1.7. Development of Tablet Compression Models

As discussed previously about the advantages of modeling, there have been various attempts in literature to develop models for pharmaceutical processes based on operation know-how and empirical results. Extensive research on processes associated with continuous manufacturing of tablets in recent times has allowed for development of first

principles models of the different unit operations, well summarized in Boukouvala et al. [53]. A more detailed idea of unit operation models along with *in silico* process control strategies that could be implemented has been reported by Singh et al. [57].

A substantial amount of work has been dedicated to understanding the compressibility of powders in the past, especially due to the application of this process in a variety of industries like metals, ceramics, catalyst, food and pharmaceuticals. Predicting compaction profiles that could lead to desirable compact characteristics by relating operating parameters to the powder properties has been the basis for most models developed in literature.

Impact of compression on particle fragmentation, deformation, and bonding, using mechanical concepts of elasticity and plasticity has been widely studied via mechanistic models developed through DEM [58] and FEM [59]. A good amount of information such as the effect of die filling, impact of tooling and particle-particle interaction on compression forces can be obtained with these models. Tablet characteristics can hence be determined and the formulation evaluated. The biggest disadvantage of these models would be the need to supply model constants and data for certain phenomena which are difficult to capture. PBM has not been used often to model this particular unit operation as compared to phenomenological semi-empirical models.

Phenomenological models have been preferred due to minimal computational time and reasonable development costs. Here, the goal has been to associate tablet characteristics (like weight, density, hardness) to operation variables (turret speed, fill depth, pre-compression length, die and punch dimensions) and incoming powder properties (bulk density, porosity). Variation in tablet weight due to die filling is related through

powder density, making it a critical property to track in the process [60]. Some of the successful endeavors of developing powder densification models can be attributed to the significant works of Shapiro, Kawakita [61] and Heckel [62]. Evolution of comprehension of powder compressibility and a comparison between Heckel and Kawakita equations has been well reviewed by Denny [63]. Though not all of these models were developed for pharmaceutical powders in particular, the equations have been modified or shown to work well with them in some cases and hence can be extrapolated.

1.7.1. Heckel Equation

The Heckel equation is based on the assumption that compression of powders is similar to a first order chemical reaction, where pores are reactants and densification of bulk is the product. It was first developed for metal powders and has now been extrapolated to different materials [62]. Equation 1, below, shows the first order relationship described by Heckel. Here, D is the relative density, K is the proportionality constant and P is the applied pressure.

$$\frac{dD}{dP} = k(1-D) \qquad \text{Equation 1}$$

This equation was integrated for relative density changing from D_0 (initial relative density) to D (final relative density), while pressure increases from zero to P (peak). This led to Equation 2.

$$Ln\left(\frac{1-D_0}{1-D}\right) = kP \qquad \text{Equation 2}$$

This equation was used to plot Heckel curves for a selection of metal powders using uniaxial compaction by Deju et al., as mentioned in Denny [63]. For certain metals such as

zinc, the graph did not depict a straight line even after the initial curved region. On the other hand, studies carried out by Duberg and Nystrom [64], with softer materials like alkali halides and sodium bicarbonates, showed Heckel plots majorly as straight lines with hardly any inflection or bend. Since, the $Ln\left(\frac{1}{1-D}\right)$ vs P curves obtained were not observed to be linear for the complete range for the selection of metal powders and did not pass through the origin, Heckel modified the equation to the following, where, *1-D* was replaced by ε (porosity), and a new parameter A was introduced.

$$Ln\left(\frac{1}{\varepsilon}\right) = kP + A \qquad \text{Equation 3}$$

Where,

$$A = Ln\left(\frac{1}{\varepsilon_0}\right) + B \qquad \text{Equation 4}$$

This helped to validate the equation for the linear part of the graphs, even though the non-linearity at lower pressures for higher initial porosities was not addressed.

Various reasons were constructed to explain the initial curvature observed in the Heckel plots. Some of the reasons put forward were [63]:

a) Particle rearrangement and settling which is difficult to quantify and hence not captured by the equation.
b) Densification of the sample by fragmentation due to brittle nature at lower pressures followed by plastic deformation at increasing compression. Though this

explanation did not seem logical enough for metal powders, it could be argued for pharmaceutical powders and softer materials.

c) Presence of agglomerates of fine powders, either due to processing to improve properties like flowability, for subsequent steps, or due to the tendency of the material to form aggregates. These aggregates, known to be weaker in strength than the particles that make them up, could be easily dismantled under slight pressure before the material started deforming.

While the relevance of these explanations was studied upon, the possibility of Heckel equation not being completely correct could not be ignored. Hence, Shapiro et al. [26] and Carstensen et al. [26], modified the existing Heckel equation to improve the predictability of the plot [65].

1.7.2. Shapiro General Compaction Equation

Shapiro general compaction equation can be seen to be an extension of the Heckel equation and includes an exponential term to capture the initial curved (non-linear) region in the Heckel profile. The Shapiro equation, just like the Heckel equation, was developed for a series of metal powders.

$$Ln\left(\frac{\varepsilon_0}{\varepsilon}\right) = kP + mP^{0.5} \qquad \text{Equation 5}$$

Here, ε is the porosity of the powder bed, whereas ε_0 is the initial porosity of the powder bed and P is the compression pressure, while k and m are parameters.

Carstensen et al. [65], modified the equation to extend its application to pharmaceutical powder formulations, that usually compress at relatively lower

compression pressures than metals. Since most of the compression data for pharmaceuticals is expected to be at pressures lower than the yield pressure (pressure at which yield strength of the material is reached), the team looked to improve the validity of the model within that pressure range. They worked with binary mixtures of pharmaceutical compounds to study and develop the model, and came up with an equation based on the fundamental idea that increase in pressure results in a decrease in powder porosity, with the assumption that this decrease is exponential.

$$Ln\left(\frac{1}{1-\varepsilon}-V_s\rho_{true}\right)=-aP+Ln(V_A\rho_{true}) \qquad \text{Equation 6}$$

Here, ρ_{true} is the true density of the powder, V_S is the actual specific solids volume, ε is the porosity, P is the compression pressure, and '*a'* is a parameter.

1.7.3. Kawakita Equation

On the other hand, Kawakita and Lüdde proposed a completely new equation that relates the compression pressure to relative change in volume of the material and works best under lower pressures for soft fluffy pharmaceutical materials [61]. The equation, popular as the Kawakita equation, was arranged as,

$$\frac{P}{C}=\frac{1}{ab}+\frac{P}{a} \qquad \text{Equation 7}$$

Where, C is the relative change in volume, and can be mathematically put as, $C=\frac{V_0-V}{V_0}$, P is the applied compression pressure, a was found to be equal to the initial porosity and b is a parameter that has to be estimated.

Singh et al. [66] have derived Equation 8 from the Kawakita equation to predict compression pressures provided we know the change in volume, initial porosity of the powder and are able to determine *b*, generally referred to as the Kawakita parameter.

$$P = \frac{(V_i - V_f)}{b(V_i(\varepsilon - 1) + V_f)} \qquad \text{Equation 8}$$

Determination of the Kawakita parameter would require the attainment of force-displacement data, every time a different formulation is studied, to be able to regress the parameter since it is formulation specific. Since pharmaceutical formulations are a complex mixture of a variety of powders, performing experiments to estimate the Kawakita parameter each time a change in composition or constituent material is made, makes the model redundant. Hence, there have been various attempts to understand and relate the effective Kawakita parameter for a formulation with Kawakita parameters of its pure constituent components. One of such studies carried out by Frenning et al., for binary mixtures of MCC (Avicel PH101) and PEG (Polyethylene glycol), led them to conclude that ideal mixing was valid for this particular system and the calculation of Kawakita parameter for the system is the weighted average of the individual components making the mixture [67]. Their idea was based on the hypothesis of addition of volumes. Relying on the same hypothesis, Mazel and his team, developed a model for prediction of reduction in volume of binary mixtures [68]. Here, they worked with MCC and L-alanine as the constituents and suggested a way to compute volume reduction under pressure using the Kawakita parameters of the pure components in the mixture rather than calculating the effective value, and the initial volume fractions [68].

Observing the analogy of Equation 7 to the fundamental law of electrical circuits, where the proportionality of voltage to current has been explained by inclusion of the proportionality constant, resistance, the Kawakita parameter can be interpreted to be the resistance to the applied compression pressure.

Table 1 below briefly describes the different compression models seen in literature over time.

Table 1. Powder compaction models.

Compaction Model	Equation	Inputs	Outputs
Heckel equation **[62]**	$Ln\left(\frac{1}{\varepsilon}\right) = kP + A$	• k • A	Compression Pressure v. Relative Density Plot
Shapiro general compaction equation	$Ln\left(\frac{\varepsilon_0}{\varepsilon}\right) = kP + mP^{0.5}$	• k • m • Initial Porosity	Compression Pressure v. Relative Density Plot; able to capture the initial non-linearity observed in the experimental data
Kawakita compression model **[61]**	$\frac{P}{C} = \frac{1}{ab} + \frac{P}{a}$	• Initial porosity • Relative change in volume • Kawakita Parameter	Peak Compression Pressure required to achieve the desired thickness
Singh's adapted Kawakita compression model **[66]**	$P = \frac{(V_i - V_f)}{b(V_i(\varepsilon - 1) + V_f)}$	• Initial Porosity • Initial Volume • Final Volume • Kawakita Parameter	Peak Compression Pressure required to achieve the desired thickness

1.8. Tablet Hardness Model

1.8.1. Kuentz and Leuenberger Hardness Model

The tablet press model described in Singh et al. [66] and implemented in gPROMS utilizes the Kuentz and Leuenberger hardness model developed for a compacted particle system to determine the tablet hardness. The Kuentz and Leuenberger equation, describes the hardness of a compact as a function of relative density and involves two parameters, namely, maximum hardness (H_{max}) and critical relative density (ρ_{rc}) [69]. This model was adapted by Singh et al. [66] as given below:

$$H_{tablet} = H_{\max}\,(1-\exp(\rho_r - \rho_{rc} + \lambda_{hard})) \qquad \text{Equation 9}$$

Where,

$$\rho_r = \frac{V_{solid}}{V_{tablet}} \qquad \text{Equation 10}$$

$$\lambda_{hard} = \log(\frac{1-\rho_r}{1-\rho_{rc}}) \qquad \text{Equation 11}$$

Maximum hardness can be defined hypothetically as the hardness at zero porosity, and critical relative density could be explained as the minimum relative density required to hold the powder with enough shear strength [69].

1.9. Objectives

As summarized above, considerable work has already been pursued with respect to compaction of powders and developing models that are able to predict force vs displacement curves. However, very little work has been done to assess the effect of material properties on compressibility. The compressibility of materials involved in a pharmaceutical formulation is extremely essential to understand, since this will help to

estimate the forces needed to make tablets of requisite standards and desired quality. Dependency of tablet physicochemical properties such as disintegration, dissolution, tensile strength and friability on compressibility, makes it a critical factor in the manufacturing operation. A lot of the problems that arise during the later stages of product development in the industry, are due to the lack of knowledge and ignorance of compressibility of pharmaceutical powders and the inability to associate its effect on some of the tablet attributes discussed previously. Detailed studies on the connection between blend characteristics and compressibility would greatly help alleviate this issue by fixing major failure possibilities (e.g. hardness and disintegration problems due to over-lubrication) during the formulation development stage.

The current dynamic tablet press model implemented in gPROMS (PSE) simulation tool is developed by Singh et al. [66]. This model adapted the Kawakita equation to determine the peak compression forces (pre-compression and main compression), and adapted Kuentz and Leueberger equation to calculate the tablet hardness (tensile strength). Additionally, the model employs material balance and other equations to relate input/output parameters and to calculate tablet weight.

Since Kawakita parameter is formulation dependent and has to be regressed every time the composition or material is varied, associating this parameter to measurable material properties would help determine this parameter for any new formulation without the need to conduct a series of experiments to collect data to help regress the constant. Therefore, this work is an attempt to understand the effect of material properties on the compaction profile and the peak compression forces observed and hence, possibly identify the Kawakita parameter as a function of these.

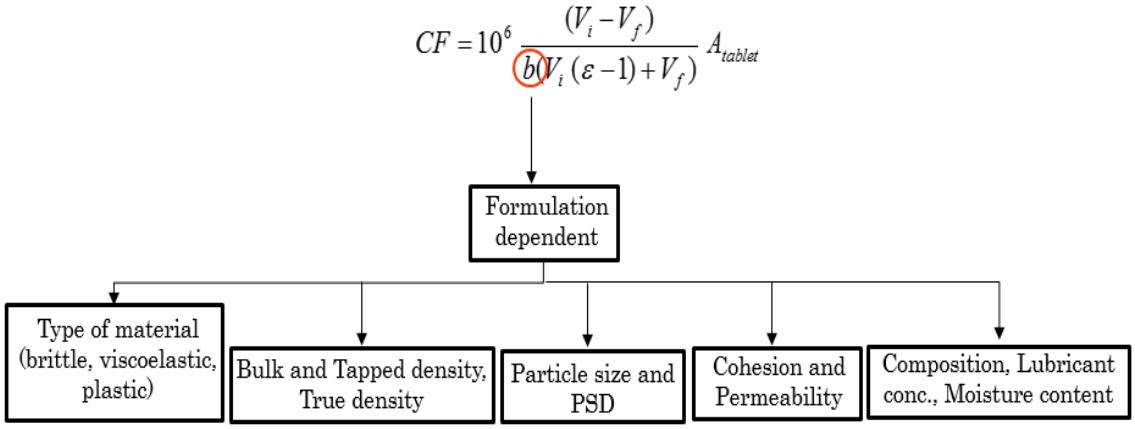

Figure 4. Dependence of Kawakita parameter on material properties.

The measurable and classifiable, material type and properties that were thought to affect compressibility have been shown in the Figure 4. Out of those mentioned, some of these properties are inter-dependent and hence all of them need not be evaluated. Also, some factors like moisture content depend on the condition (relative humidity) of the environment (here, laboratory), where the experiments were performed. Since factors like these are difficult to control, their influence was not considered in this study. The same properties mentioned above were used to develop a linear relation to determine the model parameters in the Kuentz hardness equation.

Furthermore, an attempt has been made to observe the effect of lubricant concentration on the behavior of model coefficients and notice a trend if any. Similar to studies concerned with understanding the effect of lubricant on powder and tablet properties [70], such as flowability [71], hardness, etc., this study will enhance our knowledge of lubricants and their effect on pharmaceutical processes.

CHAPTER 2

EXPERIMENTAL METHODS

2.1. Materials

The materials for the experiment were carefully selected in order to have a broad design input (material property) space. Some commonly used pharmaceutical excipients: Lactose monohydrate, two different grades of microcrystalline cellulose (MCC), and active pharmaceutical ingredient: Acetaminophen, were used with varying concentrations of lubricant, magnesium stearate. The two grades of MCC utilized were Avicel PH101 (FMC BioPolymer) and Avicel PH301 (FMC BioPolymer).

Table 2. Average bulk densities of selected excipients (Input design space).

Excipient (Trade Name)	Description	Bulk Density (g/cm^3)
Lactose	Monohydrate, Foremost® NF Lactose, 310	0.66
Avicel® PH 101	Microcrystalline Cellulose NF	0.26 – 0.31
Avicel® PH 301	Microcrystalline Cellulose NF	0.34 – 0.45

The excipients, which form the majority of any pharmaceutical formulation, and hence dramatically affect formulation properties, were chosen such that a wide range of material properties would be tested. All the excipients included in this experimental design are plastic in nature and hence, undergo compaction via plastic deformation.

A detailed description of the materials used for the study has been mentioned in Table 3.

Table 3. List of materials used for the study.

Brand Name	Material	Supplier
Paracetamol (APAP Compap 0093)	Acetaminophen	Mallinckrodt Inc.
Avicel® PH 101	Microcrystalline cellulose (MCC)	FMC BioPolymer
Avicel® PH 301	Microcrystalline cellulose (MCC)	FMC BioPolymer
Lactose	Lactose monohydrate	Foremost Farms
Magnesium Stearate	Magnesium Stearate	Mallinckrodt Inc.

2.2. Design of Experiment

The blends that were used to study the effect of material properties on compression have been described in Table 4 below.

Table 4. Blend composition.

Blend No.	API	Excipient*	Lubricant**
1	-	Lactose	0.25%
2	-	Lactose	0.75%
3	-	Lactose	1%
4	-	Lactose	1.5%
5	-	Avicel 101	0.25%
6	-	Avicel 101	0.75%
7	-	Avicel 101	1%
8	-	Avicel 101	1.5%
9	-	Avicel 301	0.25%
10	-	Avicel 301	0.75%
11	-	Avicel 301	1%
12	-	Avicel 301	1.5%
13	APAP Compap (15%)	Avicel 101	1%

**Remaining is the excipient composition, **Magnesium Stearate*

Lactose, Avicel 101, and Avicel 301, were blended at four different levels of magnesium stearate ranging from 0.25 – 1.5%. One blend of each, lactose, Avicel 101, and Avicel 301, at a particular lubricant concentration were used as internal validation points.

Blend of paracetamol (APAP Compap 0093 – Mallinckrodt) as Active Pharmaceutical Ingredient, Avicel PH101 and magnesium stearate was used as an external validation and to check if the relationship obtained could be extrapolated and applied to ternary mixtures.

The advantage of this Design of Experiment (DOE) is that it helps to not only study the effect of material properties, majorly influenced by the excipient here, on the compaction profiles, but also the influence of magnesium stearate as an additive (lubricant) on the formulation and hence, compression forces and tablet properties.

2.3. Experimental Procedures

2.3.1. Preparation of blends

All the powders were used as received. All the formulations were prepared with a target weight of 1500 g in an 8 quart capacity V-shell blender (Patterson-Kelley). Top-bottom loading format was followed for charging of the mixture components into the blender. For the binary mixtures, the excipient was loaded first, followed by the lubricant on the top. The lubricant was well spread over the excipient to ensure as uniform mix as possible. Blender speed was set at 19 RPM for a period of 2.5 mins. In case of the ternary mixture, the API (APAP Compap 0093) and excipient (Avicel PH101) were initially blended for a period of 12.5 minutes at the same speed of 19 RPM, followed by another 2.5 minutes with the lubricant (Magnesium stearate). The blending was monitored and performed in between temperatures of 25 – 29°C at a steady 10% relative humidity. The intensifier bar was not used for any of the formulations during blending, and hence it can be speculated that the shear effect is negligible and hence the coating of magnesium stearate on the excipient particles is insignificant. Additionally, intensifier bars aid with the purpose

of disintegrating agglomerates usually formed during wet granulation. Since here a direct compaction process was being followed, application of the intensifier bar was not needed.

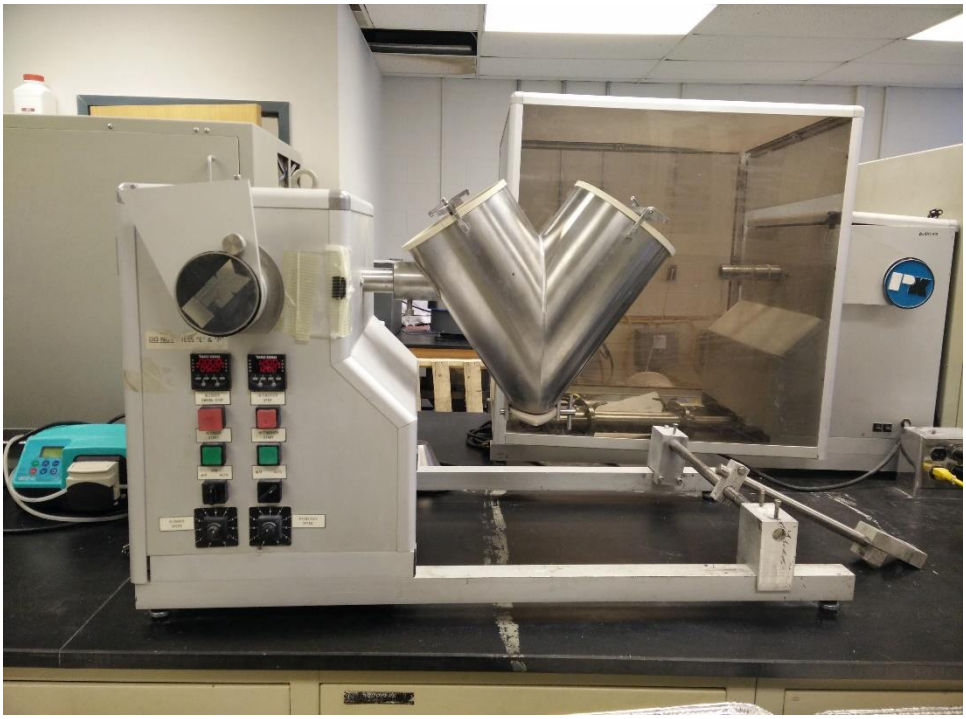

Figure 5. V-blender used for blending.

In order for the V-blender to be an effective mixing tool, the recommended fill volume is 40-60% of its capacity [72, 73]. This is to allow air space for the particles to shift, move and mix well. A fill volume of less than 20% is too small to witness substantial slipping action, the mechanism on which this blender is dependent for mixing. Hence, in order to ensure decent blend uniformity, it is advised that the fill volume is at least 25% and not more than 60%.

With 1500 g as the target blend weight, the fill volume percent of the blends could be calculated using bulk density data to check if it met the suggested requisite.

Table 5. Fill volume percent in V-blender

Blend	Volume of material (cm^3)	Fill volume percent (%)
Lactose + MgSt (0.25%)	2319.89	30.6
Lactose + MgSt (0.75%)	2250.00	29.7
Lactose + MgSt (1%)	2245.00	29.7
Lactose + MgSt (1.5%)	2320.96	30.7
Avicel 101 + MgSt (0.25%)	4295.88	56.7
Avicel 101 + MgSt (0.75%)	4102.50	54.2
Avicel 101 + MgSt (1%)	4145.83	54.8
Avicel 101 + MgSt (1.5%)	4079.29	53.9
Avicel 301 + MgSt (0.25%)	3360.00	44.4
Avicel 301 + MgSt (0.75%)	3276.25	43.3
Avicel 301 + MgSt (1%)	3226.36	42.6
Avicel 301 + MgSt (1.5%)	3307.42	43.7
APAP (15%) + Avicel 101 + MgSt (0.25%)	3790.08	50.1

2.3.2. Characterization of Blends – Analytical methods

The blends were characterized for material properties like bulk and tapped density, cohesion, permeability, compressibility and particle size distribution before making compacts using the Presster™ tablet press.

(a) Bulk and Tapped Density

Bulk and tapped density of the blends were estimated by following the standard procedure outlined in USP <616> [74]. In this process 100 g of powder was poured in a 250 ml graduated cylinder and the volume of powder was noted. The actual mass of powder (m) added was divided by the observed volume (V_0) to obtain the bulk density in g/ml. In order to estimate the tapped density of the powder formulation, the graduated cylinder was then tapped 10, 500 and 1250 and 2500 times using a Quantachrome Autotap™ tapped density analyzer. Volumes after 10, 500, 1250 and 2500 taps were recorded respectively as

V_{10}, V_{500}, V_{1250} and V_{2500}. The last volume which did not subside the volume previous to it by 2 ml was noted as the final tap volume (V_t) and was used to calculate the tapped density of the blend.

$$\rho_{bulk} = \frac{m}{V_0} \qquad \text{Equation 12}$$

$$\rho_{tapped} = \frac{m}{V_t} \qquad \text{Equation 13}$$

The bulk and tapped density calculations were used to further calculate the Hausner's ratio (H) and Carr Index (CI) and qualitatively designate the blends with their flow character. Hausner's ratio is widely used to characterize powder flow properties and can be defined quantitatively as the ratio of tapped density of a powder to its bulk density. Carr Index, on the other hand is an indication of powder compressibility and can be estimated by the equation given below.

$$H = \frac{\rho_{tapped}}{\rho_{bulk}} \qquad \text{Equation 14}$$

$$C = 100\left(\frac{H-1}{H}\right) \qquad \text{Equation 15}$$

(b) Shear Cell

The Freeman FT4 powder rheometer (Freeman technology Ltd., Worcestershire, UK) was used to perform shear cell tests to understand flow properties of the blends by determining the cohesion values for the same. FT4 powder rheometer is a universal powder tester and the shear test is an important and widely accepted characterization test for pharmaceutical powders. Shear cell test measures the shear stress of the powder observed

at different levels of the applied normal stress and this allows for plotting of the Yield Locus (line), the intersection of which with the y-axis gives the cohesion value.

For the measurements, the powder samples were gently poured into a 25 mm x 10 ml splitting cylindrical vessel. A 23.5 mm helical blade provided with the equipment was used for conditioning to remove excess air, followed by which the vessel was split and the mass automatically recorded by the computer. Since the shear cell module of 6 kPa was chosen, the powder was then consolidated at a normal pressure of 6 kPa by a 24 mm shear cell provided. As mentioned previously, the shear stress was then measured at five different applied normal stresses, quantitatively, 4, 3.5, 3, 2.5 and 2 kPa. The FT4 software then constructed the Mohr's diagram for the samples and provided the flow function and cohesion coefficients.

(c) Permeability

Permeability test is useful in measuring the resistance between particles in a powder bed and plays an important role in understanding filling behavior of materials in the die before compression. The permeability module in the FT4 powder rheometer measures the pressure drop across the powder bed. This pressure drop (ΔP) measured, along with the air flow rate used (q), viscosity of air (η) and height of powder bed (L) can be applied in the following equation to calculate the permeability of the powder blend.

$$\kappa = \frac{q\eta L}{\Delta P} \quad \text{Equation 16}$$

Here, a splitting cylindrical vessel of 25 mm x 10 ml dimension was used to run the permeability test. The splitting vessel allows for accurate mass and volume measurements

and the pressure drop across the powder bed was estimated whilst a consolidated normal stress of 15 kPa was applied.

Since all the measurements were performed around room temperature (within the temperature range of 22.7 – 27.6°C), the viscosity of air was taken to be 184.82 Pa.s (viscosity of air at 26.67°C) for the calculations. Length of powder bed was 0.51 cm and the flow rate of air was regulated at 0.2 cm/s.

(d) Compressibility

The compressibility tests are done to assess the ability of a powder to form a compact. The FT4 has a compressibility test module capable of doing measurements at varying levels of normal stress up to 15 kPa. Here, the change in volume of the powder is measured with increasing load applied via a vented piston that allows for excess air to escape. This percentage change in volume for a given normal pressure is given out as compressibility.

(e) Particle Size Analysis

Particle size distribution analysis was conducted on the Beckman Coulter LS 13 320 multi-wavelength laser diffraction particle size analyzer. The instrument uses the principles of light scattering with its patented PIDS (Polarization Intensity Differential Scattering) technology along with its Tornado powder dispersing system to measure the particle size distribution for a range of 0.017 um to 2000 um for wet or dry powder systems. The basis of this equipment is that the scattered light is unique for each particle size since the intensity of scattered light depends on the scattering angle. The scattering pattern obtained is passed through a Fourier lens that refracts the light of any particle at a specific

angle onto a particular detector, irrespective of the particle's position in space in the incident beam. This composite scattering pattern obtained for all particle sizes in the sample is measured by the detectors and de-convolved into the different particle sizes that can be observed as an output in the software, and the relative amplitude of each number is a measure of the relative volume of the equivalent spherical particles of similar size.

Since this is a disruptive method of particle size analysis, it is important to have excess material at hand for other characterization tests.

2.3.3. Compression of Blends

The blends were made into tablets on a compaction simulator known as the Presster™ (Metropolitan Computing Corporation, East Hanover, NJ). The Presster™ is a rotary tablet press replicator involving a single die and punch assembly capable of moving along a linear track, back and forth during the compression operation. It is capable of replicating a number of industrially used tablet presses such as the Fette, Kikusui and others. This ability of the equipment to mimic the environment of different tablet presses is due to the presence of different compression rolls (based on dimension) that change with each selection.

The tablets press is connected to a software which allows the user to adjust and fix the operating parameters for each run, record the values of desired variables, and generates plots such as the Heckel and Kawakita plot, force-displacement, stress-strain graphs etc., for study purposes. Some of the variables that need to be input at the start of each run are dosing position (fill depth), pre-compression position (pre-compression length) and compression position (tablet thickness desired). The sample, then has to be transferred to

the feed shoe, accurately located above the die to guide the powder. The feed shoe has been devised to move from its initial place to a temporary position during the compression and ejection stages to allow for the movement of punches in and out of the die. This movement is automatic, fast and has impeccable timing. It is recommended to run the carriage manually once, through the rolls, before starting to make tablets to check for mechanical setup errors. Following this, it is suggested that the first trial tablet be discarded and excluded from the experimental data. It is advised that this practice be followed every time an input parameter is changed or a new set of tablets with a different powder sample are going to be made. The Presster™, hence, is a versatile and complex tablet press replicator, that is friendly to operate with fair bit of practice and experience.

The set of experiments on the Presster™ were performed using the same die diameter of 8 mm for all. The fill depth and tablet thickness were varied as a 2 x 3 factorial design with the rate of tablet production kept constant. The compaction profiles and peak compression forces were recorded for each formulation. The tables of the process parameters used for each formulation can be found in Appendix 2.

2.3.4. Tablet Weight, Thickness and Hardness Measurement

A random sample of six tablets out of the ten for each operating condition for each formulation were selected for weight, thickness and hardness measurements. The thickness of the tablets were measured after a rest period of 4-5 days to allow for complete elastic expansion. A set of digital vernier calipers (Mitutoyo) was used to record tablet thickness. Following weight and thickness measurements, tablets were tested for hardness on Dr. Schleuniger® Pharmatron Manual tablet hardness tester (Model 6D). The Pharmatron allows for hardness measurement in units of Kiloponds, Newtons, Strong Cobbs, or Pounds

Apothecary. The equipment is user-friendly and the measurement procedure involves placing the tablet in between the jaws and pressing start button. The jaws close to diametrically apply pressure on the tablet and detect the corresponding break force. The break force is displayed on the screen in the units selected and shall be recorded for every tablet in the random sample as it may vary. Tablet hardness is a destructive measurement technique and should be performed last and only after other requisite measurements have been performed.

Figure 6. Schleuinger® Pharmatron tablet hardness tester (Model 6D).

CHAPTER 3

RESULTS AND DISCUSSIONS

3.1. Experimental Result

The blends were characterized for the material properties of bulk and tapped density, cohesion, permeability, compressibility, and particle size. All the tests were performed in triplicates to ensure reproducible results, except for bulk and tapped density measurements which were performed as a duplicate. The averages of the material characterization results from experiments have been reported below in Tables 6-7. The particle size analysis measurements are given in Table 8.

Table 6. Material characterization results I.

Blend	Bulk Density (g/cm^3)	Standard Deviation (g/cm^3)	Tapped Density (g/cm^3)	Standard Deviation (g/cm^3)	Hausner Ratio (-)
1	0.647	0.007	0.883	0.019	1.366
2	0.667	0.000	0.913	0.007	1.370
3	0.646	0.006	0.902	0.000	1.396
4	0.668	0.012	0.915	0.006	1.370
5	0.349	0.003	0.456	0.009	1.307
6	0.366	0.002	0.477	0.002	1.304
7	0.368	0.007	0.479	0.009	1.303
8	0.362	0.001	0.484	0.005	1.339
9	0.446	0.000	0.587	0.007	1.314
10	0.458	0.013	0.592	0.001	1.292
11	0.454	0.007	0.588	0.000	1.297
12	0.465	0.001	0.595	0.004	1.279
13	0.396	0.001	0.514	0.009	1.299

Table 7. Material characterization results II.

Blend	Cohesion (kPa)	Standard Deviation (kPa)	Pressure Drop (mbar)	Standard Deviation (mbar)	Compressibility (volume %)	Standard Deviation (volume %)
1	0.35	0.09	6.94	0.47	14.95	0.54
2	0.37	0.03	11.28	0.48	14.91	0.15
3	0.36	0.03	12.23	0.83	16.02	0.79
4	0.44	0.07	13.62	0.23	16.17	1.21
5	0.76	0.23	2.43	0.08	15.19	0.05
6	0.66	0.07	2.91	0.21	14.46	0.54
7	0.29	0.01	3.25	0.06	14.35	0.36
8	0.43	0.08	3.11	0.27	14.14	0.37
9	0.35	0.02	3.71	0.09	13.26	0.19
10	0.47	0.32	3.87	0.03	13.91	0.16
11	0.17	0.04	4.5	0.12	13.93	0.71
12	0.60	0.51	4.92	0.31	13.34	0.33
13	0.44	0.08	1.21	0.01	12.85	0.31

Table 8. Blend particle size analysis results.

Blend	Mean (µm)	D10 (µm)	D50 (µm)	D90 (µm)	Standard Deviation (µm)
1	55.05	11.48	55.69	96.94	31.31
2	53.31	9.57	53.65	96.29	31.90
3	49.31	8.47	49.84	89.33	29.91
4	49.18	7.81	48.90	91.34	31.03
5	71.06	21.20	66.23	129.63	39.46
6	66.24	17.41	62.61	119.87	37.30
7	69.27	17.47	66.13	123.85	39.21
8	56.60	13.18	55.99	99.34	31.50
9	59.01	16.29	55.87	106.87	32.78
10	53.72	13.95	51.92	95.72	30.27
11	49.82	12.53	49.04	88.26	28.00
12	51.94	12.13	49.88	94.33	30.38
13	65.71	16.42	63.22	116.93	36.94

3.2. Data Analysis and Regression

3.2.1. Principal Component Analysis

Principal Component Analysis was performed using a statistical software, Minitab 17 (Minitab). The objective of performing a PCA was to segregate the blends on the basis of material properties and understand the operating material design space we would be using to build the model. PCA helps to be able to conclude patterns in this high dimension data set by reducing the variables of interest into smaller set of components. These components are able to express majority of the variability observed in the actual results. A correlation PCA was performed with the material characterization and particle size results obtained since these measured variables are different physical quantities and hence, they need to be standardized and rescaled. The Eigen values of the correlation matrix given in Appendix 4 indicate that taking the first two components would help capture sufficient variability (87.3%) and hence reduce the dimension of our data set from 9 to 2. Figure 7, also known as the scree plot, is a graphical representation of the Eigen values for each component present in Appendix 4.

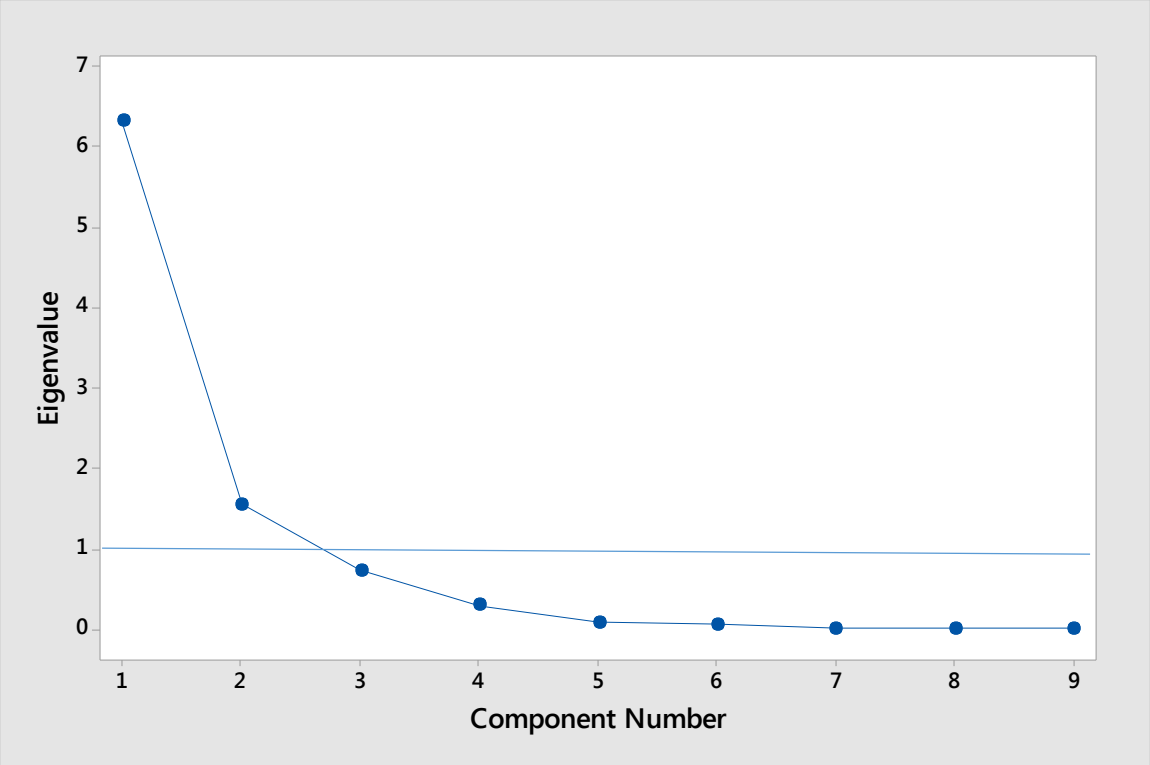

Figure 7. Scree Plot generated during PCA.

The Eigen value analysis in Table 29 of Appendix 4 lists the correlations between each variable (i.e. material property) and each principal component. These correlations help interpret the influence of each variable on the principal components. From the correlation values, it can be concluded that PC1 (Principal Component 1) is strongly affected by bulk density, tapped density, pressure drop and particle size of the blend since the absolute values for these variables are higher than that of others. Similarly, PC2 (Principal Component 2) is strongly correlated to compressibility and cohesion. PC1 can be seen to increase with decrease in bulk density, tapped density and pressure drop (since these are negatively correlated) and increase in particle size (since this is positively correlated). For PC2, both cohesion and compressibility are negatively correlated, hence

an increase in any leads to a decrease in PC2. This analysis can be used to explain the distribution of scores in Figure 8.

Lactose, Avicel 101 and Avicel 301 have magnesium stearate as lubricant at four levels of 0.25%, 0.75%, 1% and 1.5%. From the score plot shown in Figure 8, we can conclude that magnesium stearate does not significantly affect the measured properties for lactose and Avicel 301. However, the lubricant concentration seems to influence the properties of Avicel 101. This is because, as we can concur from the plot that the excipient scores for lactose and Avicel 301 are closely knit to each other, whereas the scores for Avicel 101 are distributed further apart, especially along PC2 axis. This distribution of scores for Avicel 101 along the PC2 axis can be attributed to the difference in properties of compressibility and cohesion among its blends. The scores for lactose and Avicel 301 are both slightly distributed along PC1 and PC2 axis showing a minor difference in material properties between the excipient blends. On the other hand, it can be observed that the excipient types affect the material characteristics vastly. This is due to the fact that the scores of different excipients are further apart on the plot. Thus we can conclude that the excipient, which is majority in quantity, dictates the material properties as compared to the lubricant, except for Avicel 101. The effect of APAP in a mixture of Avicel 101 and magnesium stearate is not impactful in terms of variation in material properties, since the score lies within the distributed group of Avicel 101. The operating material design space can be seen to be governed by the extreme points in the score plot. Since, the validation points lie within or in proximity of the design space, suitable prediction of model coefficients for these points is expected.

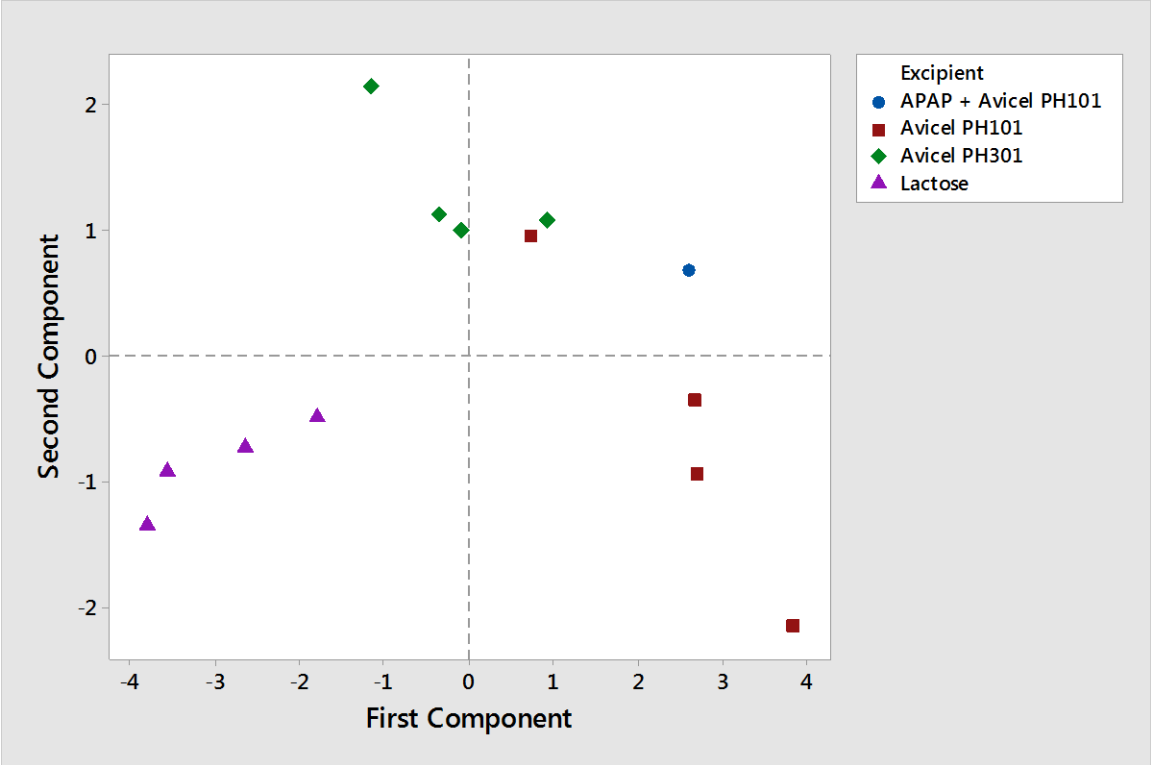

Figure 8. Score plot of the measured blend properties.

3.2.1. Regression of model coefficients

(a) Pre-compression and main compression parameters

The initial porosity was calculated using bulk and true density of the blends as shown in Equation 17 [75].

$$\varepsilon_0 = 1 - \left(\frac{\rho_{true}}{\rho_{bulk}} \right) \qquad \text{Equation 17}$$

The bulk density of the blends was measured whereas the true density for the blends was calculated as a weighted average via Equation 18, using the true densities of individual components obtained from literature.

$$\rho_{true}^{mix} = \rho_{true}^{A} \left(\frac{w_A}{w_A + w_B} \right) + \rho_{true}^{B} \left(\frac{w_B}{w_A + w_B} \right) \qquad \text{Equation 18}$$

The true densities of the materials used in the experiment have been reported in Table 9.

Table 9. True densities of materials used in the experiment.

Material (-)	True Density (g/cm^3)	Reference (-)
Lactose	1.54	[76]
Microcrystalline cellulose	1.547	[77]
Acetaminophen (APAP)	1.293	-
Magnesium Stearate	1.092	[78]

The initial porosity of the blends were calculated as mentioned above and given in Table 10.

Table 10. Calculated blend initial porosities.

Blend (-)	Calculated Initial Porosity (-)
1	0.58
2	0.57
3	0.58
4	0.56
5	0.77
6	0.76
7	0.76
8	0.77
9	0.71
10	0.70
11	0.71
12	0.70
13	0.74

The Kawakita parameter as explained earlier is a constant that aids in adjusting the value of compression force. Separate values for pre-compression force and main compression force were obtained via regression with the help of experimental data from the Presster since pre-compression and main compression forces work in different ranges

with respect to the relative density. Non-linear regression was performed using the solver tool in Excel 2013 to regress the compression parameters. The pre-compression force observed was in the range of 0.3 – 1.3 kN and the main compression force was in the range of 0.2 – 24 kN overall.

The regressed parameters and initial porosities for the blends have been reported along with R^2 (correlation) and RMSE (Root Mean Square Error) values in Table 11. The correlation values for the pre-compression and main compression forces are in the range of 0.573 – 0.965 and 0.617 – 0.986 respectively, mainly on the higher side, thus showing good agreement between the model and experimental data. In addition the RMSE values show that the model is able to convincingly predict the compression forces using the regressed parameters.

Table 11. Regressed pre-compression and main compression Kawakita parameters with the initial porosities used.

Blend (-)	**Kawakita Parameter (MPa^{-1})**		**Correlation (-)**		**Force (kN)**	
	Regressed Parameter		**R^2**		**RMSE**	
	Pre-compression	**Main compression**	**Pre-compression**	**Main compression**	**Pre-compression**	**Main compression**
1	0.0555	0.0412	0.965	0.964	0.106	1.067
2	0.0518	0.0322	0.944	0.939	0.105	1.203
3	0.0602	0.0263	0.741	0.828	0.121	2.345
4	0.0526	0.0237	0.859	0.617	0.098	3.528
5	0.1445	0.0278	0.573	0.943	0.060	1.317
6	0.1512	0.0373	0.629	0.981	0.052	0.771
7	0.1529	0.0382	0.865	0.939	0.050	1.533
8	0.1581	0.0398	0.800	0.885	0.057	2.157
9	0.1246	0.0563	0.925	0.952	0.049	1.627
10	0.1177	0.0382	0.849	0.986	0.048	0.772
11	0.1218	0.0342	0.756	0.897	0.047	2.021
12	0.1164	0.0318	0.899	0.800	0.056	3.179
13	0.1457	0.0389	0.864	0.943	0.047	1.653

The plots in Figure 9 are a comparison of the model output to the experimental data for the regressed values of the Kawakita parameters for main compression force. These plots for Avicel 101, lactose, and Avicel 301, all at 0.75% magnesium stearate concentration, and APAP + Avicel 101 with 1% lubricant show a good agreement between the model and experimental data for the compression forces. The plots also observe the variation in compression force with fill depth and tablet thickness. This shows that the material in application significantly affects the compression process parameters which influences the process output.

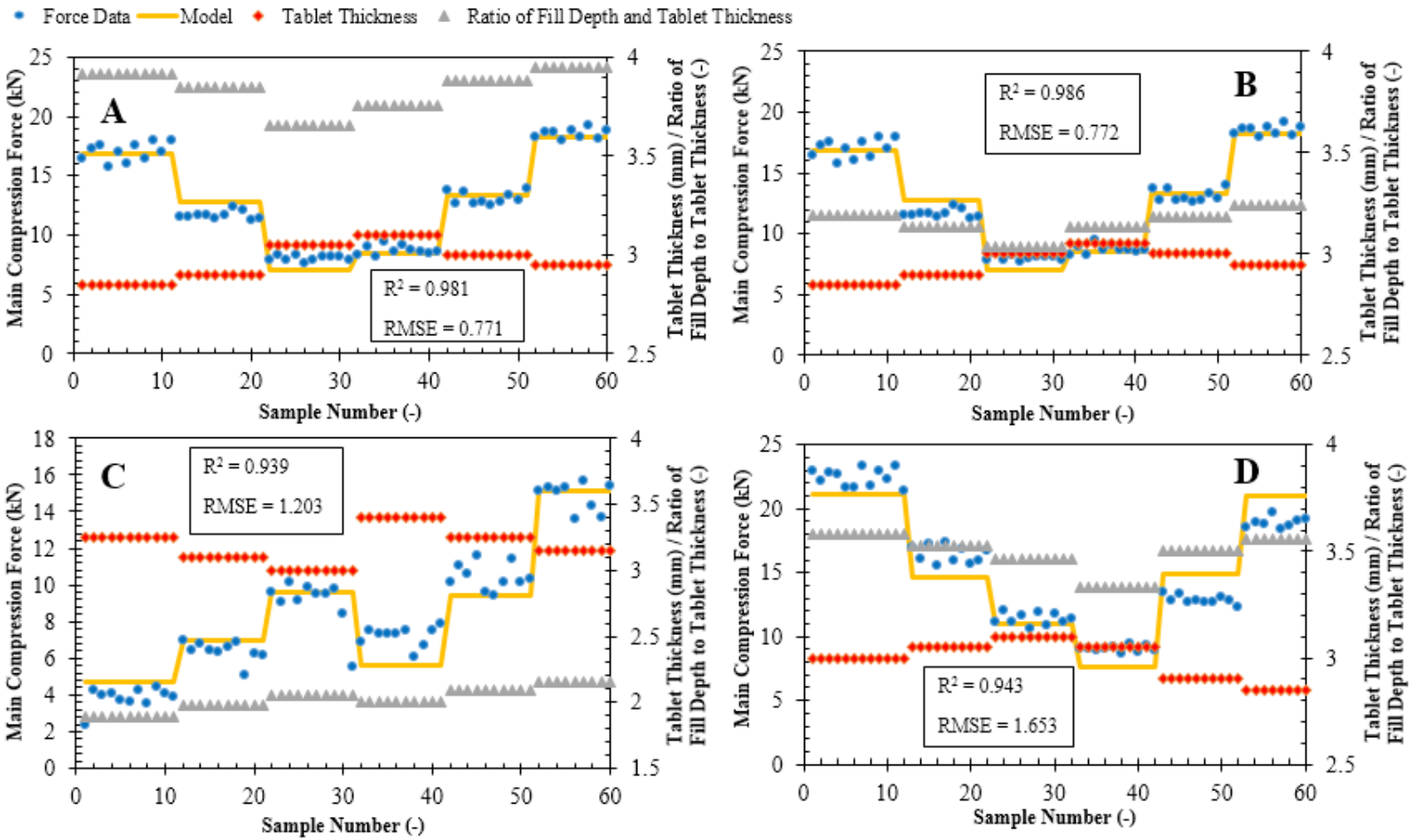

Figure 9. Comparison between experimental data and model output for main compression force obtained using regressed Kawakita parameters with variation in fill depth and tablet thickness set points for (a) Avicel 101 with 0.75% MgSt (b) Avicel 301 with 0.75% MgSt (c) Lactose with 0.75% MgSt (d) APAP (15%) + Avicel 101 with 1% MgSt.

Additionally, parity plots for main compression force for all the blends have been included in Appendix 1 for reference to show the agreement between model output and experimental values.

The effect of magnesium stearate concentration on Kawakita parameter for pre-compression and main compression was studied for the three excipients: Lactose, Avicel 101, and Avicel 301. There was only a slight variation in the Kawakita parameter for pre-compression for all the three excipient blends at different magnesium stearate concentrations. Since pre-compression force is utilized to remove excess air between the particles and does not contribute directly to bonding of particles to form the final compact, the variation in pre-compression force among the same excipient blends was observed to be insignificant. This could be the reason why the force adjusting pre-compression Kawakita coefficient seemed to change only marginally. The small variation in pre-compression parameter with lubricant concentration could be due to change in material properties of the system.

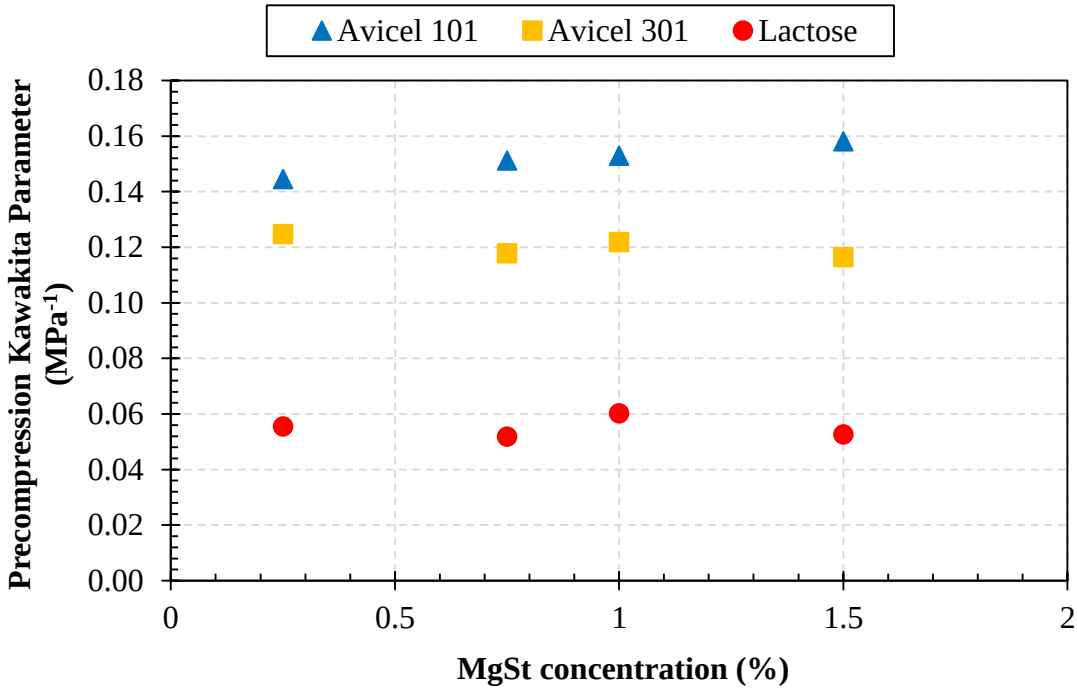

Figure 10. Effect of magnesium stearate concentration on kawakita parameter for pre-compression.

On the other hand, it can be observed from the plot (see Figure 11) that the main compression parameter for lactose and Avicel 301 decreases with increasing magnesium stearate concentration, whereas, the parameter increases in case of Avicel 101. As we know from Equation 8 the kawakita parameter and compression pressure are inversely proportional to each other. This means that higher compression pressure is required for lactose and Avicel 301 with increasing lubricant concentration. This could be attributed to the fact that increasing magnesium stearate concentration leads to coating of particles resulting in reduced surface area available for inter-particle bonding of excipient molecules. On the other hand, the opposite trend observed for Avicel 101 maybe due to the

difference in material properties such as bulk density and cohesion of this powder system compared to lactose and Avicel 301.

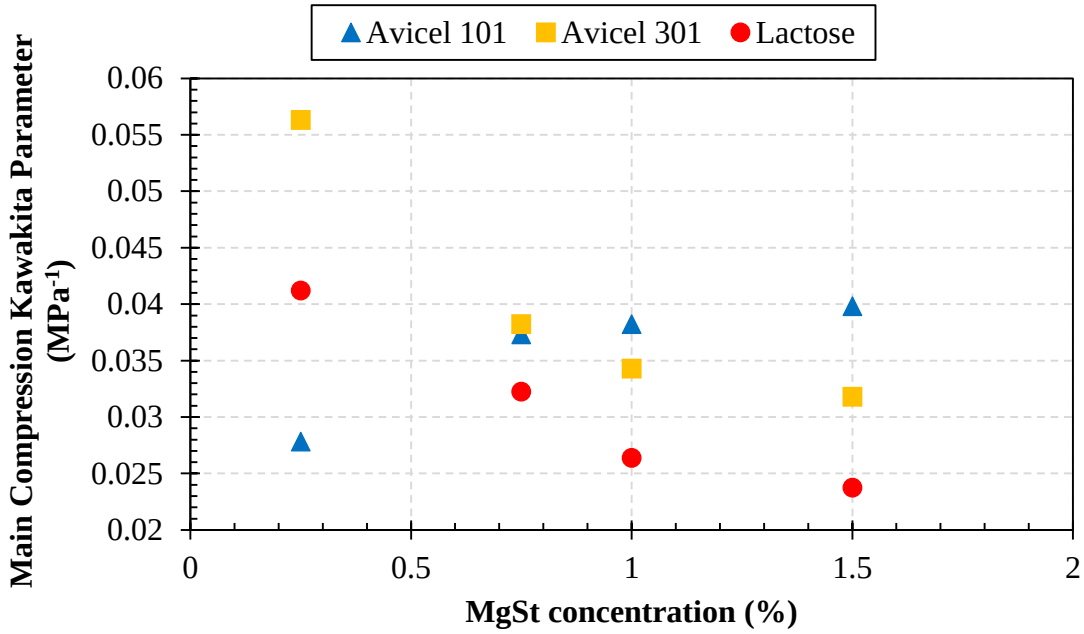

Figure 11. Effect of magnesium stearate concentration on kawakita parameter for main compression.

(b) Maximum hardness and critical relative density

Maximum hardness parameter and critical relative density in the Kuentz and Leuenberger equation were regressed simultaneously by minimizing the sum square error between the model output and the experimental data. Trends within similar materials with changing magnesium stearate concentration were studied for both the model parameters.

Here, the break force recorded as a result from the hardness tester was converted to tensile strength, since the hardness of a tablet refers to the tensile strength of the compact. Regression for maximum hardness and critical relative density was performed in Excel.

The regression results along with the corresponding R^2 (coefficient of determination) and RMSE values have been tabulated below.

Table 12. Hardness model regressed parameters.

Blend (-)	Regressed Parameters		Correlation (-)	Hardness (MPa)
	Critical Relative Density (-)	Maximum Hardness (MPa)	R^2	RMSE
1	0.799	4.462	0.935	0.324
2	0.808	4.312	0.965	0.197
3	0.847	4.530	0.946	0.276
4	0.844	4.260	0.959	0.239
5	0.622	16.727	0.968	0.365
6	0.656	15.188	0.987	0.204
7	0.620	17.000	0.951	0.604
8	0.626	12.595	0.960	0.263
9	0.703	12.110	0.984	0.214
10	0.682	10.336	0.963	0.213
11	0.672	9.354	0.950	0.202
12	0.659	8.705	0.940	0.205
13	0.646	10.541	0.973	0.165

Figure 12 show the plots for tablet tensile strength with varying tablet relative density and compares the model output to the measured value. Trendline have been shown to depict the power nature of tensile strength and relative density. The plots show a very good agreement between model and experimental data with R^2 value greater than 0.93 for all the different blends.

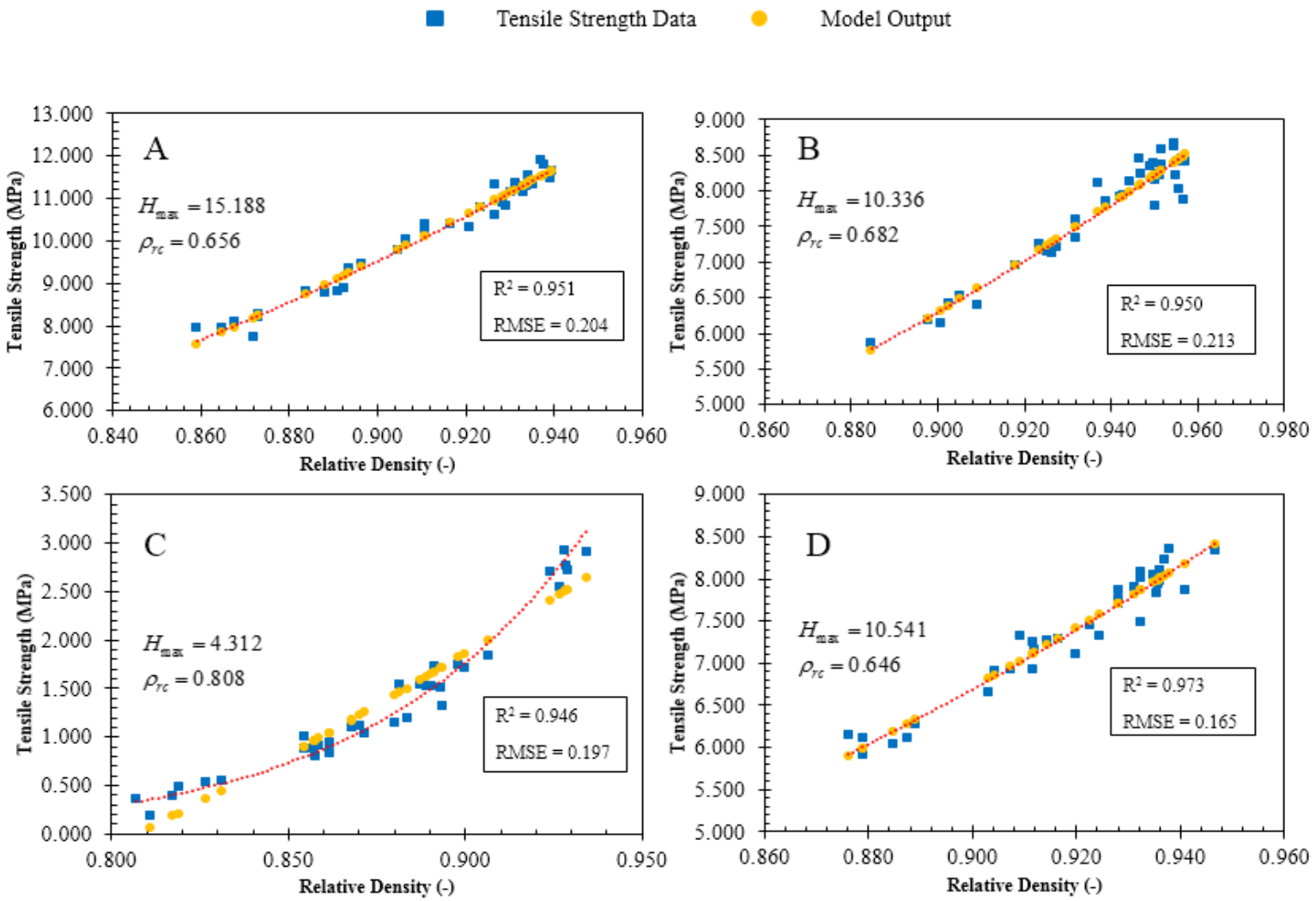

Figure 12. Comparison between tensile strength data and model output for varying tablet relative densities for (a) Avicel 101 with 0.75% MgSt (b) Avicel 301 with 0.75% MgSt (c) Lactose with 0.75% MgSt (d) APAP (15%) + Avicel 101 with 1% MgSt.

The effect of magnesium stearate concentration on maximum hardness and critical relative density can be observed in Figure 13. The maximum hardness for Avicel 101 and Avicel 301 can be interpreted to decrease with increasing lubricant concentration, except for the deviation of Avicel 101 with 1% MgSt. This decrease in maximum hardness is same as the expected decrease in tensile strength of tablets with increasing lubricant surface area and can be attributed to the fact that coating of excipient particles with lubricant reduces the surface area for inter-particle bonding [70, 71]. The deviation for Avicel 101 with 1% MgSt may be ignored as an outlier in this case. On the other hand, a constant maximum hardness is observed for lactose with changing magnesium stearate concentration. This difference from microcrystalline cellulose could be due to difference in material properties, which might have affected the coating of particles with the lubricant.

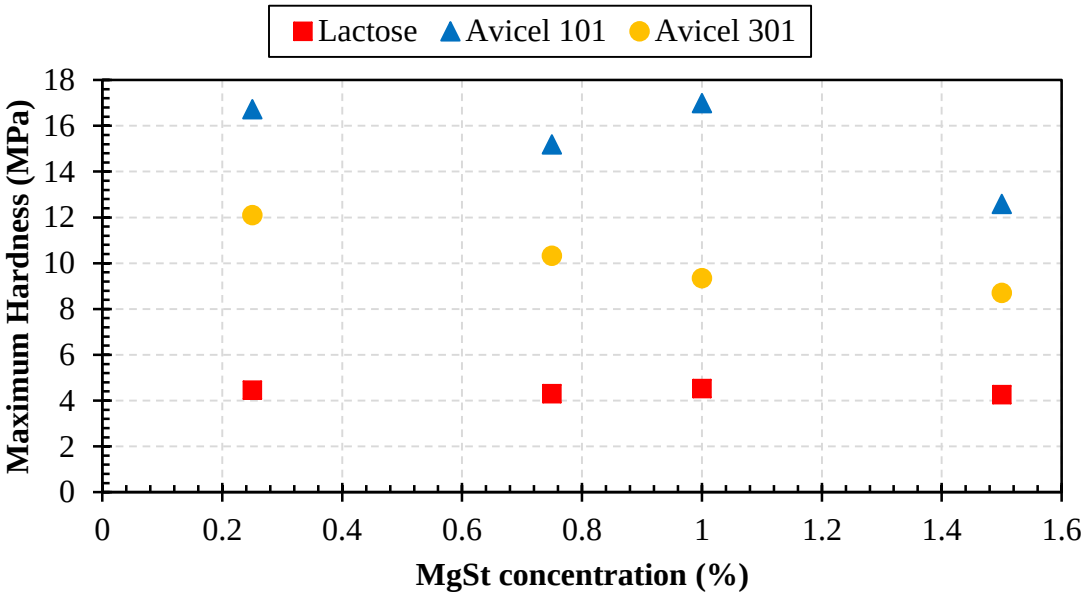

Figure 13. Effect of magnesium stearate concentration on maximum hardness.

Theoretically, critical relative density can be expected to increase with increase in lubricant concentration. This is because, as hardness of the compressed powder system decreases with increasing magnesium stearate concentration, the minimal density required to hold the powder as a compact will increase. However, from Figure 14, only lactose and Avicel 101 seem to follow the trend expected. The critical relative density of Avicel 301, on the other hand, is seen to decrease with larger quantities of magnesium stearate. The change in critical relative is only marginal for all the three excipients and this could be since small concentrations of magnesium stearate does not notably affect the relative density of the blends, and hence might not drastically affect the critical relative densities as well.

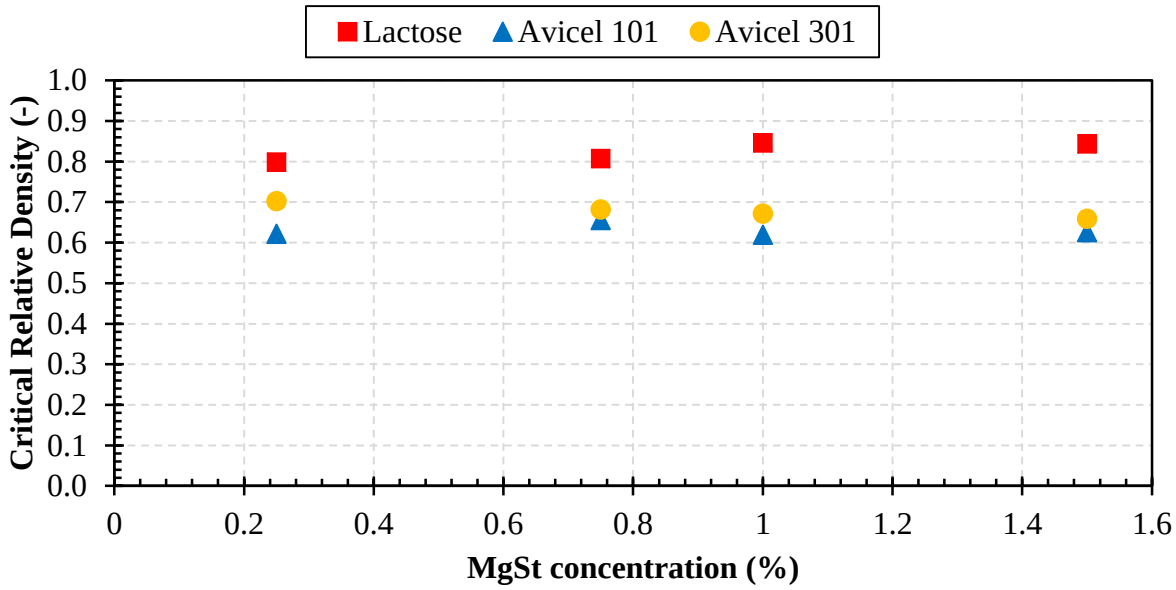

Figure 14. Effect of magnesium stearate concentration on critical relative density.

3.2.2. Partial Least Squares Regression

PLS regression works to minimize the squared error between the data and functions used to predict the data, and thus helps to improve the predictability of the regressed model. Since the objective here was to develop a model that would be able to predict the data with the functions desired with fair accuracy, regression via least squares was selected. Non-linear regression may help improve the accuracy of prediction further, but would come at a significant cost of using iterative optimization techniques to estimate the unknown parameters. Additionally, iterative optimizations usually require a reasonable initial value of the parameters to converge at a solution. Since the knowledge of the behavior of model coefficients with respect to each material property is limited, use of non-linear regression would be complex and may not be feasible. Therefore, the model coefficients were associated to the material properties measured via a regressed linear model.

A general PLS linear model is represented as Equation 19. Here, a_0 is the constant, whereas a_i is the coefficient of i^{th} function, X_i, and Y is the response.

$$Y = a_0 + \sum_{i=1}^{9} a_i X_i \qquad \text{Equation 19}$$

(a) Kawakita parameter for precompression and main compression

The regressed values of the kawakita parameter for pre-compression and main compression were used for partial least squares regression to obtain a correlation between the regressed values and the blend material properties. Only the three blends involving lactose, Avicel 101, and Avicel 301 at three different magnesium stearate concentrations of 0.25, 1 and 1.5% were used to fit the regressed model. The blends at 0.75% concentration

of magnesium stearate was used as internal validation, and the APAP and Avicel 101 mixture was utilized as an external validation.

The partial least squares regression was performed on Minitab 17 and the results generated have been given in Appendix 4. Equations 20 and 21 below are the regressed linear models obtained for the prediction of Kawakita parameters for pre-compression and main compression, respectively.

$$b(PCF) = 0.2435 - 0.1724(\rho_{bulk}) - 0.1189(\rho_{tapped}) - 0.0198(\sigma) \\ -0.001147(\Delta P) + 0.005145(\Delta V) - 0.000102(\mu) - 0.00016(D10) \\ -0.00028(D50) - 0.00008(D90) \quad \text{Equation 20}$$

Figure 15 plots the standardized coefficients for each predictor (material property) considered in the PLS model for the pre-compression parameter. These plots have been obtained as a result of the PLS regression performed in Minitab 17.

Table 13 describes the material property corresponding to the predictor variable in the standardized coefficient plots.

Table 13. Predictor variables.

Predictor Variable (-)	Material Property (-)
1	Bulk Density
2	Tapped Density
3	Cohesion
4	Pressure Drop
5	Compressibility
6	Mean Particle Size
7	D10
8	D50
9	D90

As we can see from Figure 15, the pre-compression Kawakita parameter is strongly affected by bulk density, tapped density, and compressibility among other properties. This is because the standardized coefficients associated with these properties are substantially higher as compared to others. Standardized coefficients ignore the units of the independent variables, which are different in this case, and hence aid in making comparisons easy. The negative signs ahead of the coefficients for bulk and tapped density depict their inverse relation to the pre-compression Kawakita parameter, i.e. when either of these two properties increases in value, the pre-compression Kawakita parameter will decrease. Since the pre-compression Kawakita parameter is inversely proportional to pre-compression pressure, an increase in bulk or tapped density will require a higher pre-compression force, which is the case. A powder system with higher density will require higher compression pressures to compress the same amount of material over the same volume.

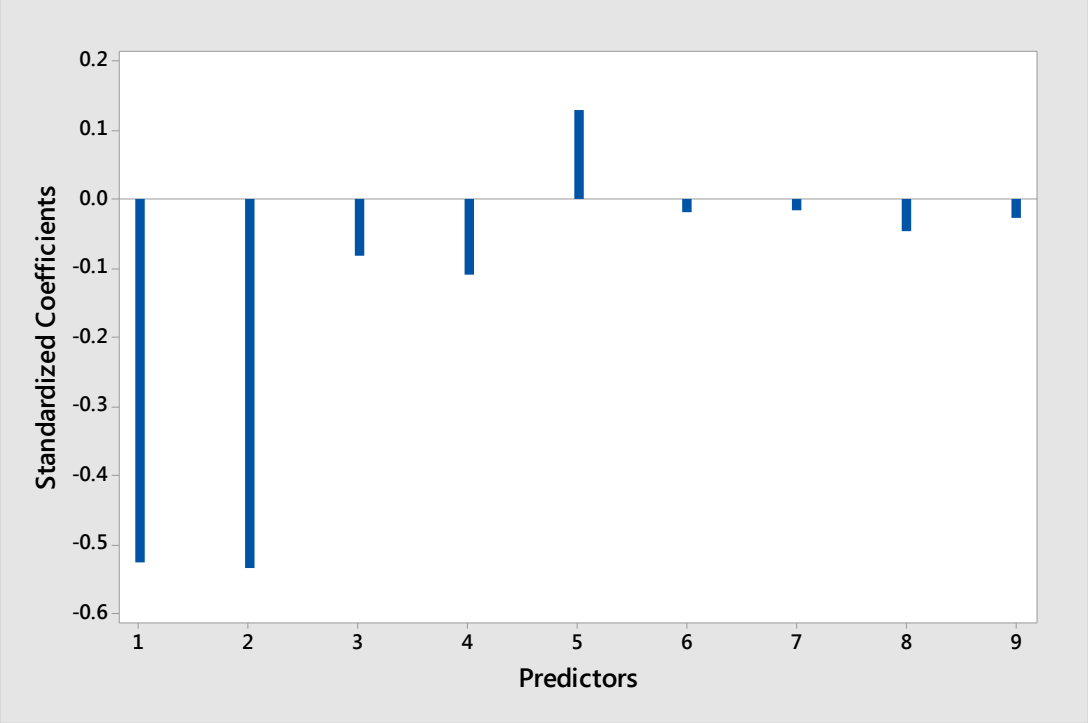

Figure 15. Standardized regression coefficients plot for the pre-compression PLS model.

Equation 16 depicts the linear relation between the original blend properties and the main compression Kawakita parameter. According to Figure 22, the main compression Kawakita parameter, seems to be strongly influenced by bulk density, tapped density, and compressibility, among other material properties. Standardized coefficients refer to the number of standard deviations by which a response variable will change with increase in one standard deviation of the predictor variable. Therefore, Figure 22 helps identify the most influential predictors of the main compression Kawakita parameter. Since the main compression stage is involved will actual compression of the powder system to form a compact, strong influence of compressibility of the material seems practical.

$$b(MCF) = 0.0934 - 0.0038(\rho_{bulk}) - 0.0233(\rho_{tapped}) - 0.0185(\sigma)$$
$$-0.00075(\Delta P) + 0.0079(\Delta V) - 0.000166(\mu) - 0.000573(D10) \quad \text{Equation 21}$$
$$-0.00025(D50) - 0.000061(D90)$$

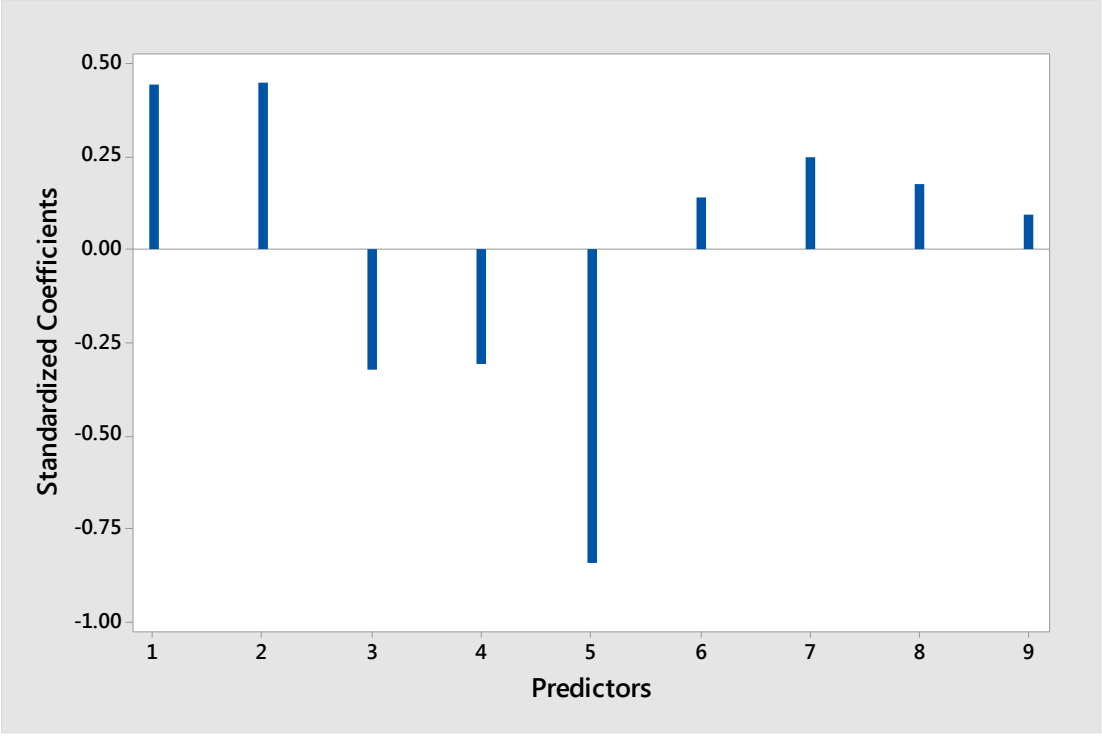

Figure 16. Standardized regression coefficients plot for the main compression PLS model.

The parity plot in Figure 17 and 18 compare the predicted value of pre-compression main compression kawakita parameter obtained from the Equation 20 and 21, respectively, to its fitted value. The plots show good correlation between the two values for three excipients with varying magnesium stearate concentrations, as well as for the internal and external validations for both pre-compression and main compression parameters. Thus, we can conclude that the linear regression model is able to predict the pre-compression and main compression Kawakita parameter with decent accuracy.

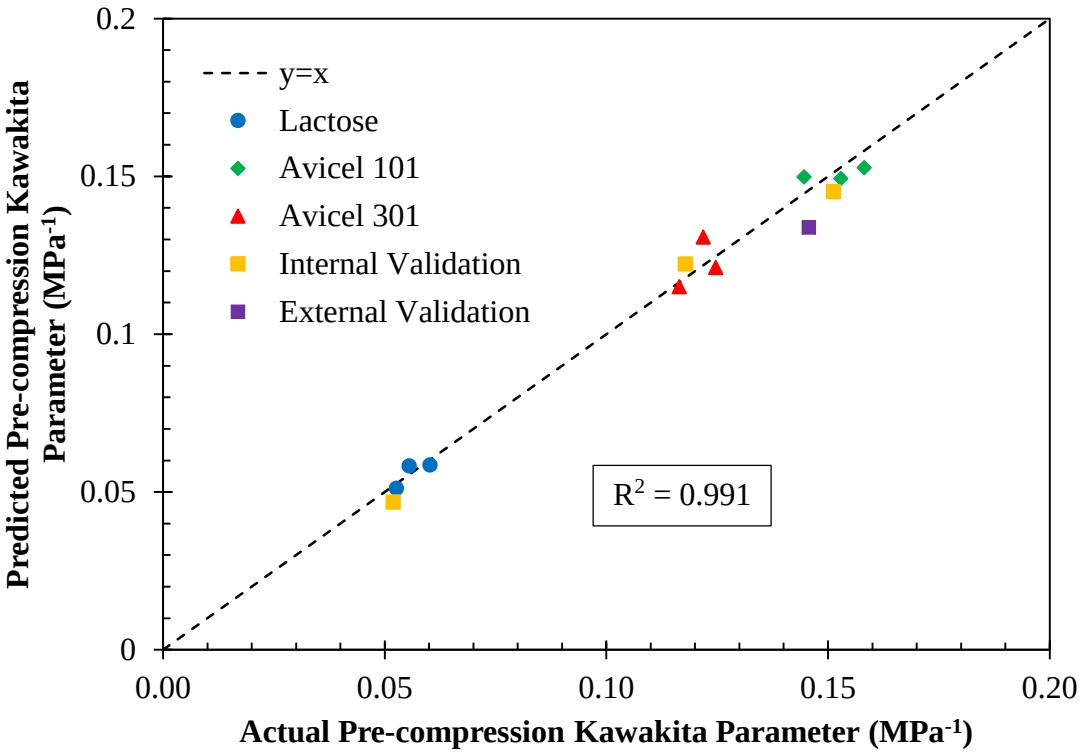

Figure 17. Parity plot between predicted and regressed kawakita parameter.

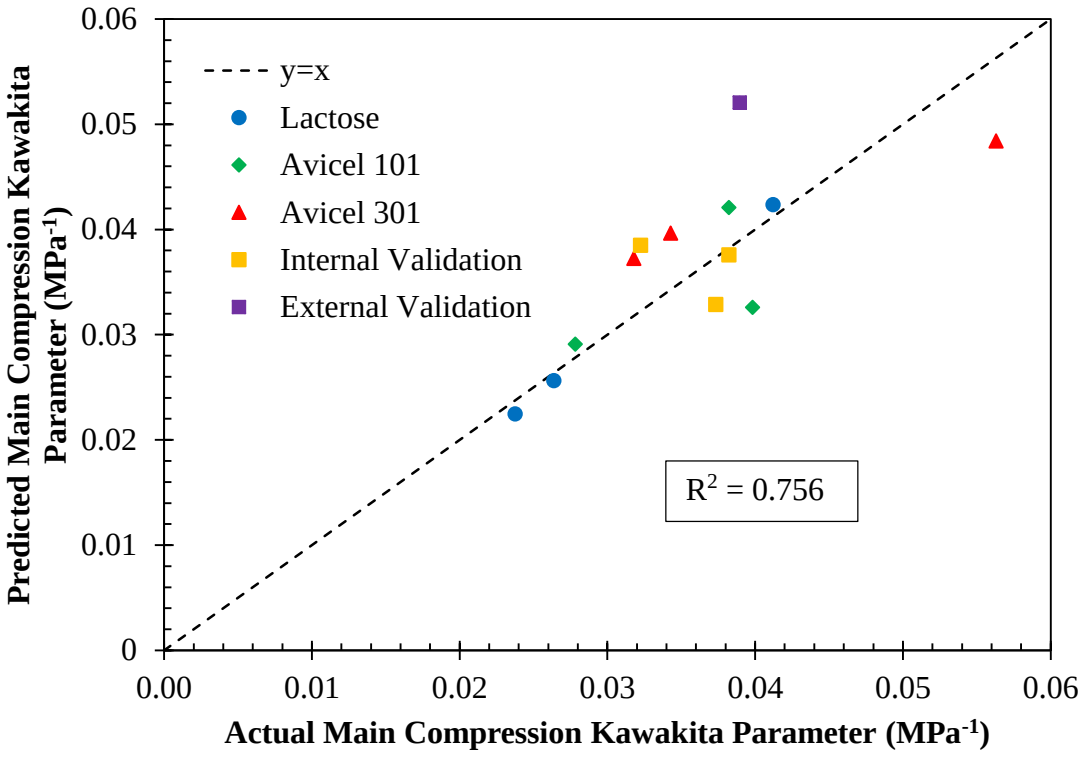

Figure 18. Parity plot between predicted and regressed kawakita parameter.

(b) Maximum hardness

Partial least squares regression was performed to obtain a linear relation that can be used to predict the maximum hardness from the material properties measured (i.e. bulk and tapped density, pressure drop, cohesion, compressibility and particle size). Here, the blends involving lactose, Avicel 101, and Avicel 301 at 0.25, 0.75 and 1.5% magnesium stearate concentrations were used to fit the regressed model. The blends at 1% lubricant concentration was used as internal validation, and the ternary mixture of APAP, Avicel 101 and magnesium stearate was used as an external validation.

Equation 22 shows the linear equation obtained via PLS associating material properties to maximum hardness.

$$H_{\max} = 9.425 - 16.169(\rho_{bulk}) - 11.013(\rho_{tapped}) - 4.374(\sigma) + 0.0231(\Delta P) + 0.365(\Delta V) + 0.0728(\mu) + 0.273(D10) - 0.118(D50) + 0.094(D90)$$ Equation 22

Here, again, bulk and tapped density seem to be the most influential properties from Figure 19, followed by D90 and D10.

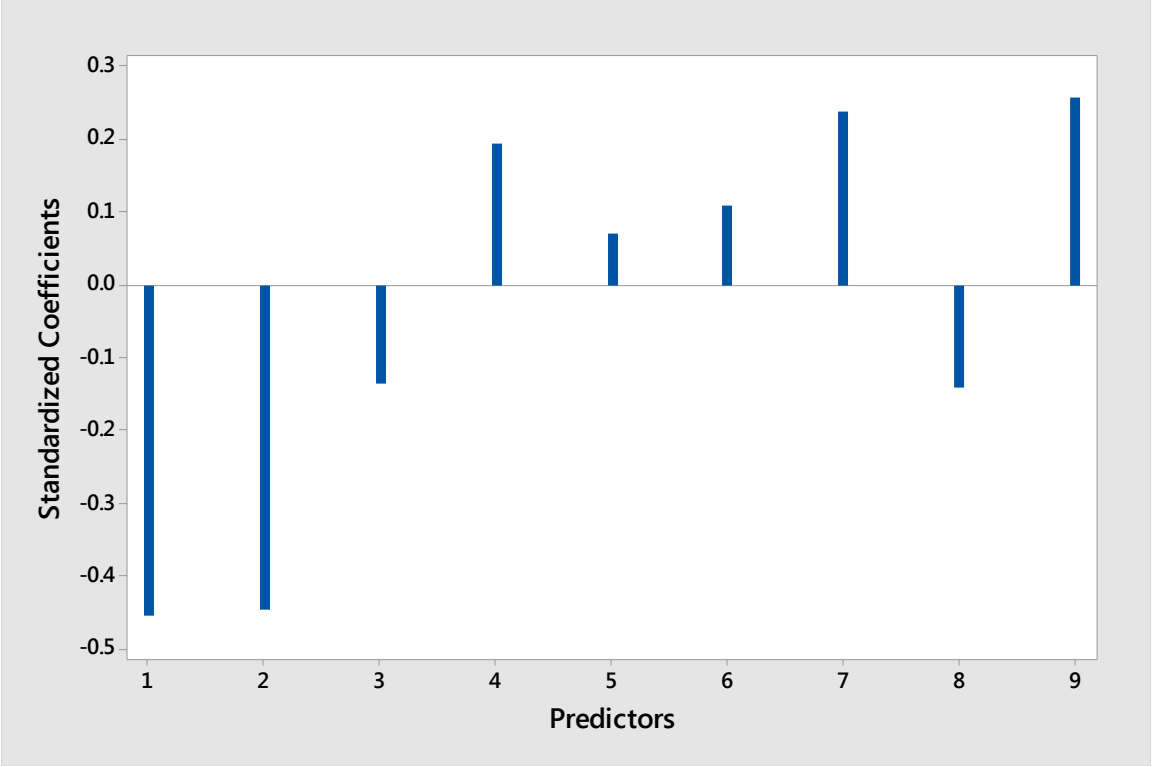

Figure 19. Standardized regression coefficients plot for maximum hardness PLS model.

The parity plot in Figure 20 compares the predicted value of maximum hardness parameter obtained from the Equation 22 to its fitted value. The plot shows a good correlation between the two values for all the blends along with the internal and external verification points.

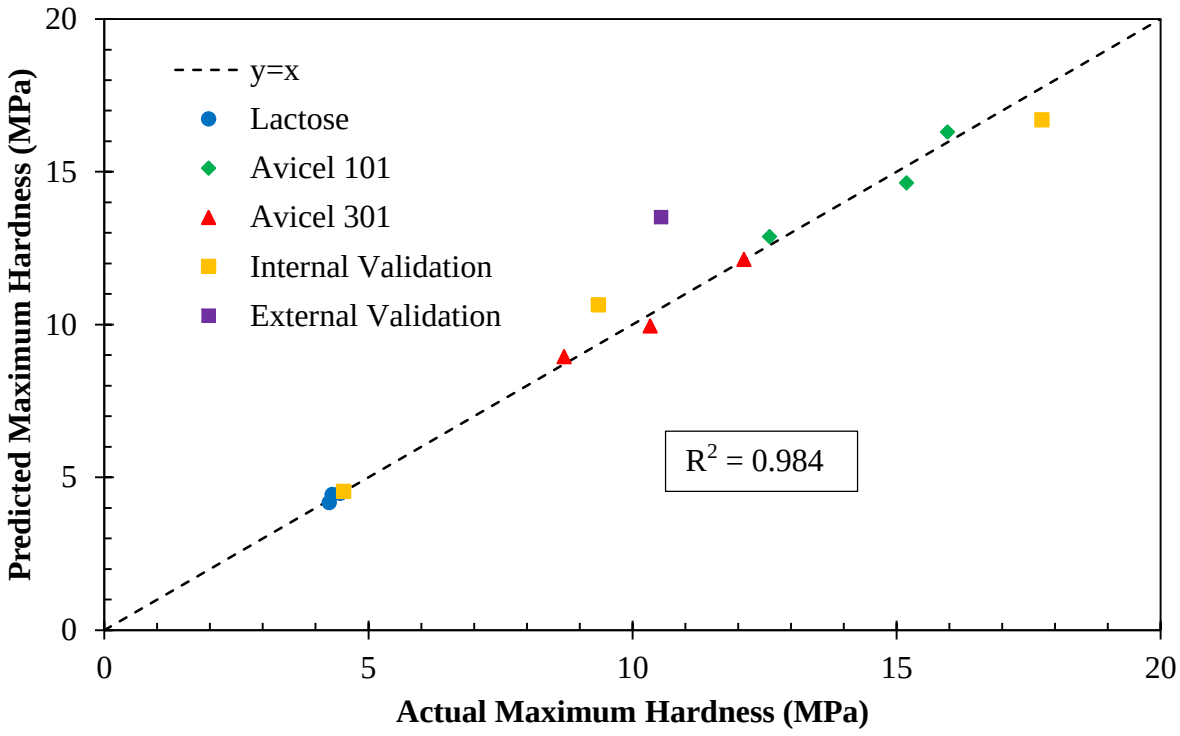

Figure 20. Parity plot between predicted and regressed maximum hardness.

Equation 23 shows the linear equation obtained via PLS for the prediction of critical relative density as part of the Kuentz hardness model.

$$\rho_{rc} = 0.2898 - 0.1546(\rho_{bulk}) - 0.1091(\rho_{tapped}) - 0.062(\sigma) + 0.0046(\Delta P) + 0.00201(\Delta V) - 0.00013(\mu) - 0.0017(D10) + 0.00023(D50) + 0.000043(D90) \quad \text{Equation 23}$$

Figure 21 compares the standardized coefficients for the predictors of the critical relative density model. The plot suggests bulk and tapped density as the most influential properties for critical relative density, followed by permeability and compressibility.

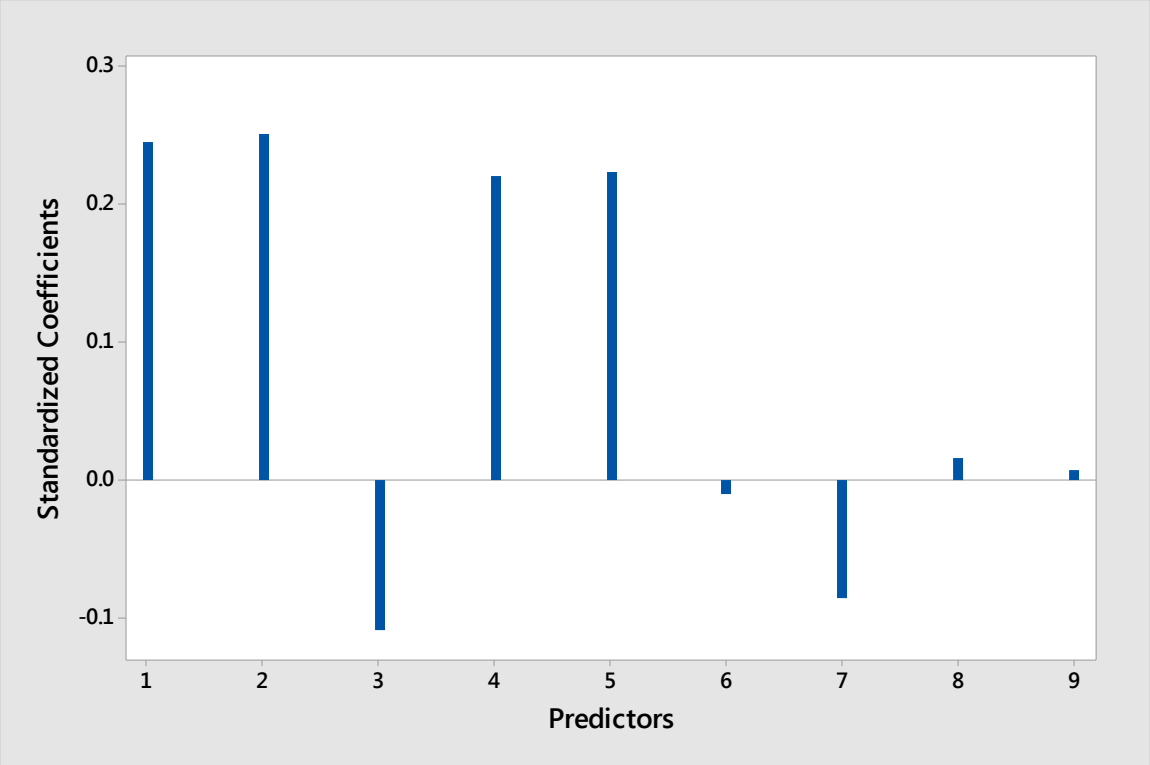

Figure 21. Standardized regression coefficients plot for critical relative density PLS model.

Figure 22 compares the predicted and fitted values of critical relative density and shows a very good agreement between the two values for all the blends and the validation points.

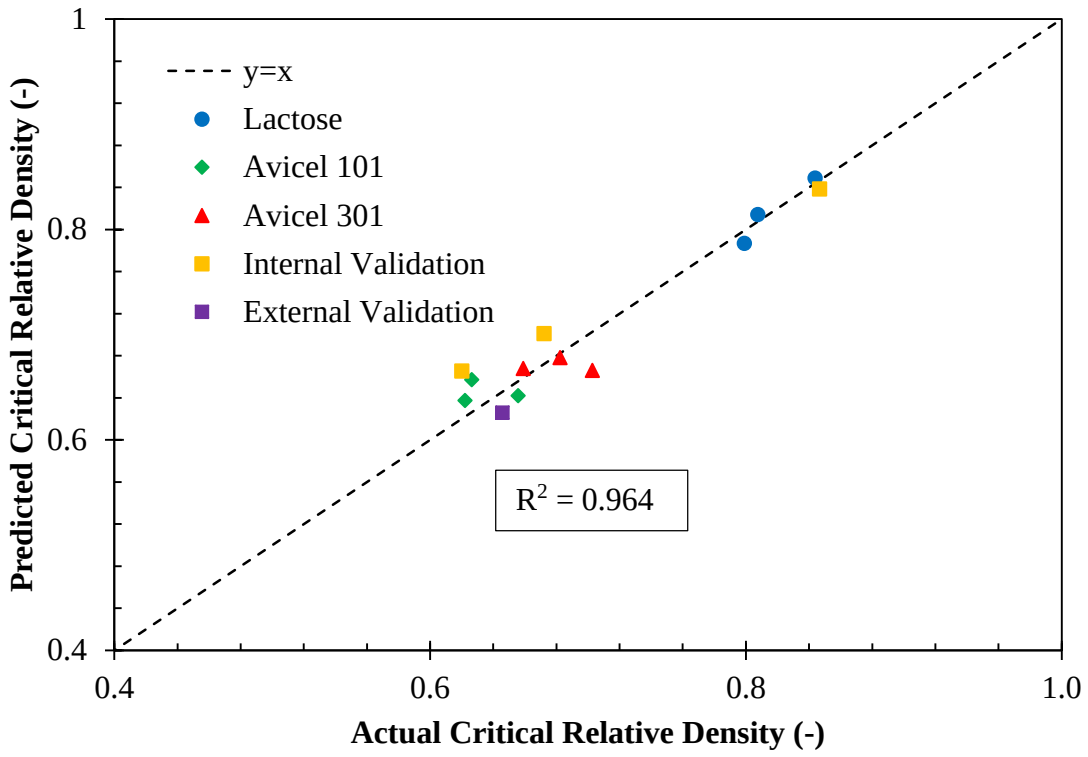

Figure 22. Parity plot between predicted and regressed critical relative density.

Summary of the regression models relating material properties to the response variables have been given below in Table 13. The table provides the coefficients associated with each material property in the linear model for each response variable when represented as Equation 19.

Table 14. Summary of the regression models relating material properties to response variables.

Model Variables (units)	Constant Coefficient Parameter	Response Variable			
		Pre-compression Kawakita Parameter (b in MPa^{-1})	Main Compression Kawakita Parameter (b in MPa^{-1})	Maximum Hardness (H_{max} in MPa)	Critical Relative Density (ρc)
Constant (as response)	a0	0.2345	0.0934	9.425	0.2898
Bulk Density (g/ml)	a1	-0.1724	– 0.0338	– 16.169	– 0.1546
Tapped Density (g/ml)	a2	-0.1189	– 0.0233	– 11.013	– 0.1091
Cohesion (kPa)	a3	-0.0198	– 0.0185	– 4.374	– 0.062
Pressure Drop (mbar)	a4	-0.001147	– 0.0075	0.0231	0.0046
Compressibility (%)	a5	0.005145	– 0.0079	0.365	0.00201
Mean Particle Size (µm)	a6	-0.000102	0.000166	0.0728	0.00013
Particle D10 (µm)	a7	-0.00016	0.000573	0.273	0.0017
Particle D50 (µm)	a8	-0.00028	0.00025	– 0.118	0.00023
Particle D90 (µm)	a9	-0.00008	0.000061	0.094	0.000043

Figure 23 shows the normalized coefficient values for each variable involved in predicting the response variables: main compression Kawakita parameter, maximum hardness, and critical relative density. The plot summarizes our conclusion of the PLS regression by estimating the most influential material properties with respect to the model coefficients. The normalized coefficient values suggest that bulk and tapped density, along with cohesion play the most crucial role in predicting the responses of the model coefficients studied. The effect of particle size on the model coefficients can be concluded to be negligible from the respective normalized coefficients in the plot. Hence, it would be interesting to check the robustness of this methodology by eliminating particle size as a predictor in PLS models developed for new set of materials with contrasting properties in the future.

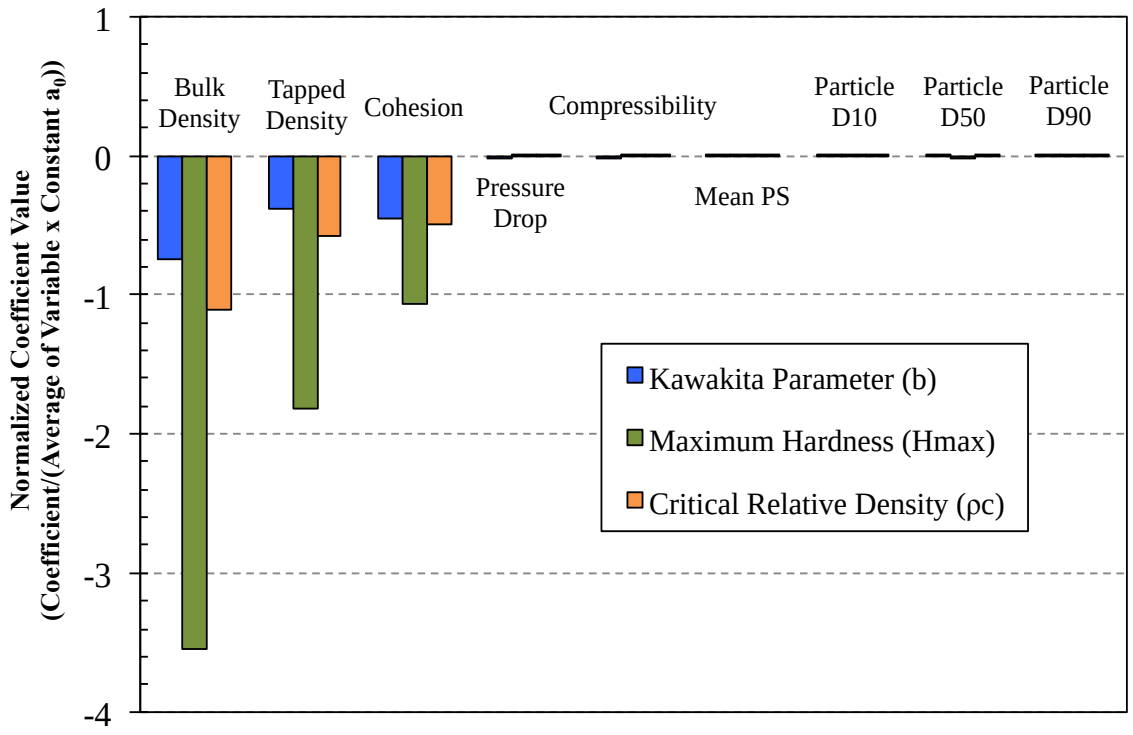

Figure 23. Normalized coefficient plot for main compression Kawakita parameter, maximum hardness and critical relative density.

CHAPTER 4

CONCLUSIONS AND FUTURE WORK

In this research, the effect of material properties on compressibility of commonly used pharmaceutical powders was studied. The design of experiment implemented helped generate experimental data to achieve the objective of the study to develop a methodology to correlate blend material properties to process parameters. The regressed linear models for both compression and hardness parameters were developed and validated for internal validation points. For the external validation point, the model showed better prediction of the hardness parameters than compression parameters. This can be observed from the parity plots that compare the actual coefficient to the PLS model estimated coefficient. In addition to developing the concept of predicting model coefficients with material properties, the effect of lubricant on the behavior of model coefficients was studied as well. Trends were observed for the response in the model coefficients (Kawakita parameter for pre-compression and main compression, maximum hardness, and critical relative density) with varying lubricant concentration. Though these seemed theoretically convincing for most of the blends, certain deviations were observed. The deviations were possibly due to the differences in material properties observed among the blends and in certain case were absolute outliers.

The results obtained indicate that correlations between material properties and semi-empirical model coefficients are feasible provided we are working within the operating material properties design space, and it is possible to predict the response of model coefficients with adequate accuracy. Such studies aid in development of process

models to predict process performance *in silico*, thereby reducing the need for experimentation. This proof of concept can aid in process development, especially in the area of design space characterization and robustness analysis. Overall, the work can be used as a basis for correlating material properties to semi-empirical models of other unit operations involved in continuous pharmaceutical processing in the future. Furthermore, the work can be expanded with other materials lying outside of the design space currently studied.

The PLS regression model obtained as a result of this work would further be implemented in the tablet press model (Equations detailed in Appendix 5) developed on gPROMS at the Engineering Research Center for Structured Organic Particulate Systems (ERC-SOPS), Rutgers University, with limitations on the validity of the model. The model could then only be applied specifically for blends involving materials used to develop it.

REFERENCES

1. Reuters, T. *Global pharma sales to reach $1.3 trillion*. 2015; Available from: http://thomsonreuters.com/en/articles/2015/global-pharma-sales-reach-above-1-trillion.html.
2. Unit, T.E.I., *Global outlook: Healthcare*. 2014.
3. (WHO), W.H.O. *Global Health Observatory (GHO) data*. Available from: http://www.who.int/gho/mortality_burden_disease/life_tables/situation_trends_text/en/.
4. Chen, L. *The Most Profitable Industries In 2015*. Investing 2015; Available from: http://www.forbes.com/sites/liyanchen/2015/09/23/the-most-profitable-industries-in-2015/#59626b087712.
5. Development, T.C.f.t.S.o.D., *BACKGROUNDER: How New Drugs Move through the Development and Approval Process*. 2001.
6. FDA, U.S., *Comparison of NMEs approved in 2010 to previous years - New Molecular Entity 2010 statistics.* 2010.
7. Scannell, J.W., et al., *Diagnosing the decline in pharmaceutical R&D efficiency.* Nat Rev Drug Discov, 2012. **11**(3): p. 191-200.
8. Coopers, P., *From vision to decision Pharma 2020*. 2012.
9. Administration, U.S.F.a.D. *Facts about Generic Drugs*. 2015 2015, June 19; Available from: http://www.fda.gov/Drugs/ResourcesForYou/Consumers/BuyingUsingMedicineSafely/UnderstandingGenericDrugs/ucm167991.htm.
10. Emanuel, J.H.B.E.J., *The Patents-Based Pharmaceutical Development Process - Rationale, Problems, and Potential Reforms.* JAMA, 2005. **294**(16): p. 2075-2082.
11. J. A. DiMasi, L.F., A. Seckler, A. Wilson, *Trends in risks associated with new drug development: success rates for investigational drugs.* Clinical Pharmacology & Therapeutics, 2010. **87**(3): p. 272-277.
12. Richard M. Felder, R.W.R., *Elementary Principles of Chemical Processes*. 2005: John Wiley & Sons, Inc.
13. Woodcock, J. *Modernizing Pharmaceutical Manufacturing – Continuous Manufacturing as a Key Enabler*. in *MIT-CMAC International Symposium on Continuous Manufacturing of Pharmaceuticals*. 2014. Cambridge, MA: Center for Drug Evaluation and Research, FDA.
14. U.S. Department of Health and Human Services, F.a.D.A., *U.S. Guidance for Industry: Q7A good manufacturing practice guidance for active pharmaceutical ingredients*, F.a.D. Administration, Editor. 2001: Rockville, MD.
15. Myerson, A.S., et al., *Control Systems Engineering in Continuous Pharmaceutical Manufacturing May 20–21, 2014 Continuous Manufacturing Symposium.* Journal of Pharmaceutical Sciences. **104**(3): p. 832-839.
16. Reinhardt, U.E., *Perspectives On The Pharmaceutical Industry.* Health Affairs, 2001. **20**(5): p. 136-149.
17. Rogers, A.J., A. Hashemi, and M.G. Ierapetritou, *Modeling of Particulate Processes for the Continuous Manufacture of Solid-Based Pharmaceutical Dosage Forms.* Processes, 2013. **1**: p. 67-127.

18. Ting, N., *Dose Finding in Drug Development*. Statistics for Biology and Health. 2006, New York: Springer.
19. Throckmorton, D., *Statement to the House of Representatives, Subcommittee on Health, Committee on Energy & Commerce "Examining Drug Shortages and Recent Effort to Address Them"*. 2014, February 10.
20. Lee, S.L., et al., *Modernizing Pharmaceutical Manufacturing: from Batch to Continuous Production.* Journal of Pharmaceutical Innovation, 2015. **10**(3): p. 191-199.
21. Plumb, K., *Continuous Processing in the Pharmaceutical Industry: Changing the Mind Set.* Chemical Engineering Research and Design, 2005. **83**(6): p. 730-738.
22. Buchholz, S., *Future manufacturing approaches in the chemical and pharmaceutical industry.* Chemical Engineering and Processing: Process Intensification, 2010. **49**(10): p. 993-995.
23. *Engineering Research Center for Structured Organic Particulate Systems*. 2006; Available from: http://ercforsops.org/.
24. *Novartis-MIT Center for Continuous Manufacturing*. Available from: https://novartis-mit.mit.edu/.
25. Schaber, S.D., et al., *Economic Analysis of Integrated Continuous and Batch Pharmaceutical Manufacturing: A Case Study.* Industrial & Engineering Chemistry Research, 2011. **50**(17): p. 10083-10092.
26. Allison, G., et al., *Regulatory and Quality Considerations for Continuous Manufacturing May 20–21, 2014 Continuous Manufacturing Symposium.* Journal of Pharmaceutical Sciences, 2015. **104**(3): p. 803-812.
27. Chatterjee, S. *FDA Perspective on Continuous Manufacturing*. in *IFPAC Annual Meeting*. 2012. Baltimore, MD.
28. Brookings, C.f.H.P.a., *Promoting Continuous Manufacturing in the Pharmaceutical Sector Discussion Guide*. 2015, October 19.
29. Stephen Byrn, M.F., Hayden Thomas, Eric Jayjock, Nicola Maron, Robert F. Meyer, Allan S. Myerson, Michael P. Thien, Bernhardt L. Trout. *Achieving Continuous Manufacturing for Final Dosage Formation: Challenges and How to Meet Them*. in *Continuous Symposium*. 2014, May 20-21.
30. Ierapetritou, M., et al., *Model-Predictive Design, Control, and Optimization.* Pharmaceutical Technology, 2013. **37**(6).
31. FDA, U.S., *Guidance for Industry PAT – A Framework for Innovative Pharmaceutical Development, Manufacturing and Quality Assurance.*, F.a.D.A. U.S. Department of Health and Human Services, Editor. 2004: Rockville, MD.
32. Rogers, A. and M. Ierapetritou, *Challenges and Opportunities in Pharmaceutical Manufacturing Modeling and Optimization*, in *Computer Aided Chemical Engineering*, J.D.S. Mario R. Eden and P.T. Gavin, Editors. 2014, Elsevier. p. 144-149.
33. Demetri P. Petrides, A.K., Pericles T. Lagonikos, *The Role of Process Simulation in Pharmaceutical Process Development and Product Commercialization.* International Society of Pharmaceutical Engineering, 2002, January/February. **22**(1).

34. Krist V Gernaey, A.E.C.-P., John M Woodley, *Development of continuous pharmaceutical production processes supported by process systems engineering methods and tools.* Future Medicinal Chemistry, 2012. **4**(11).
35. M. Sebastian Escotet-Espinoza, R.S., Maitraye Sen, Thomas O'Connor, Sau Lee, Sharmista Chatterjee, Rohit Ramachandran, Marianthi Ierapetritou, Fernando Muzzio, *Flowsheet Models Modernize Pharmaceutical Manufacturing Design and Risk Assessment.* Pharmaceutical Technology, 2015. **39**(4).
36. Singh, R., et al., *A systematic framework for onsite design and implementation of a control system in a continuous tablet manufacturing process.* Computers & Chemical Engineering, 2014. **66**: p. 186-200.
37. McKenzie, P., et al., *Can pharmaceutical process development become high tech?* AIChE Journal, 2006. **52**(12): p. 3990-3994.
38. Markarian, J., *Using Model-Predictive Design in Solid-Dosage Manufacturing Processes.* Pharmaceutical Technology, 2013. **37**(6).
39. Enterprise, P.S.; Available from: http://www.psenterprise.com/.
40. AspenTech. Available from: https://www.aspentech.com/.
41. Anselmo Buso, M.G., *Mathematical Modeling in Chemical Engineering: A Tool to Analyse Complex Systems*, in *Numerical Simulations of Physical and Engineering Processes*, J. Awrejcewicz, Editor. 2011, September, InTech.
42. Matzopoulos, M., *Dynamic process modeling: Combining models and experimental data to solve industrial problems.* 2011.
43. Ketterhagen, W.R., M.T. am Ende, and B.C. Hancock, *Process Modeling in the Pharmaceutical Industry using the Discrete Element Method.* Journal of Pharmaceutical Sciences, 2009. **98**(2): p. 442-470.
44. Verkoeijen, D., et al., *Population balances for particulate processes—a volume approach.* Chemical Engineering Science, 2002. **57**(12): p. 2287-2303.
45. Sen, M., et al., *Multi-dimensional population balance modeling and experimental validation of continuous powder mixing processes.* Chemical Engineering Science, 2012. **80**: p. 349-360.
46. Barrasso, D. and R. Ramachandran, *A comparison of model order reduction techniques for a four-dimensional population balance model describing multi-component wet granulation processes.* Chemical Engineering Science, 2012. **80**: p. 380-392.
47. Ramsey, J.L., *Between the Fundamental and the Phenomenological: The Challenge of 'Semi-Empirical' Methods.* Philosophy of Science, 1997. **64**(4): p. 627-653.
48. Kremer, D.M. and B.C. Hancock, *Process Simulation in the Pharmaceutical Industry: A Review of Some Basic Physical Models.* Journal of Pharmaceutical Sciences, 2006. **95**(3): p. 517-529.
49. Trucano, T.G., et al., *Calibration, validation, and sensitivity analysis: What's what.* Reliability Engineering & System Safety, 2006. **91**(10-11): p. 1331-1357.
50. Gao, Y., F.J. Muzzio, and M.G. Ierapetritou, *A review of the Residence Time Distribution (RTD) applications in solid unit operations.* Powder Technology, 2012. **228**: p. 416-423.
51. Fogler, H.S., *Elements of chemical reaction engineering*. 2006.

52. David Amsallem, C.F. *Reduced Order Modeling*. Available from: https://web.stanford.edu/group/frg/active_research_themes/reducedmodel.html.
53. Boukouvala, F., et al., *An integrated approach for dynamic flowsheet modeling and sensitivity analysis of a continuous tablet manufacturing process.* Computers & Chemical Engineering, 2012. **42**: p. 30-47.
54. Gernaey, K.V. and R. Gani, *A model-based systems approach to pharmaceutical product-process design and analysis.* Chemical Engineering Science, 2010. **65**(21): p. 5757-5769.
55. Davies, P., *Oral Solid Dosage Forms*, in *Pharmaceutical Preformulation and Formulation*, M. Gibson, Editor. 2009, Informa Healthcare USA, Inc.: New York, NY. p. 367-430.
56. Pharmacopeia, U.S., *General Chapter <1151> Pharmaceutical Dosage Forms*. 2009.
57. Singh, R., M. Ierapetritou, and R. Ramachandran, *An engineering study on the enhanced control and operation of continuous manufacturing of pharmaceutical tablets via roller compaction.* Int J Pharm, 2012. **438**(1-2): p. 307-26.
58. Jerier, J.F., et al., *Study of cold powder compaction by using the discrete element method.* Powder Technology, 2011. **208**(2): p. 537-541.
59. Zavaliangos, A., et al., *Temperature Evolution during Compaction of Pharmaceutical Powders.* Journal of Pharmaceutical Sciences, 2008. **97**(8): p. 3291-3304.
60. Mehrotra, A., et al., *A modeling approach for understanding effects of powder flow properties on tablet weight variability.* Powder Technology, 2009. **188**(3): p. 295-300.
61. Kawakita, K. and K.-H. Lüdde, *Some considerations on powder compression equations.* Powder Technology, 1971. **4**(2): p. 61-68.
62. Heckel, R.W., *Density-Pressure Relationships in Powder Compaction.* Transactions of The Metallurgical Society of AIME, 1961. **221**(671-675).
63. Denny, P.J., *Compaction equations: a comparison of the Heckel and Kawakita equations.* Powder Technology, 2002. **127**(2): p. 162-172.
64. Duberg, M. and C. Nyström, *Studies on direct compression of tablets XVII. Porosity—pressure curves for the characterization of volume reduction mechanisms in powder compression.* Powder Technology, 1986. **46**(1): p. 67-75.
65. Cartensen, J.T., J.M. Geoffroy, and C. Dellamonica, *Compression characteristics of binary mixtures.* Powder Technology, 1990. **62**(2): p. 119-124.
66. Singh, R., K.V. Gernaey, and R. Gani, *ICAS-PAT: A software for design, analysis and validation of PAT systems.* Computers & Chemical Engineering, 2010. **34**(7): p. 1108-1136.
67. Frenning, G., J. Nordström, and G. Alderborn, *Effective Kawakita parameters for binary mixtures.* Powder Technology, 2009. **189**(2): p. 270-275.
68. Mazel, V., et al., *Original predictive approach to the compressibility of pharmaceutical powder mixtures based on the Kawakita equation.* International Journal of Pharmaceutics, 2011. **410**(1–2): p. 92-98.
69. Martin Kuentz, H.L., *A new model for the hardness of a compacted particle system, applied to tablets of pharmaceutical polymers.* Powder Technology, 2000. **111**: p. 145-153.

70. Wu, J.L.a.Y., *Lubricants in Pharmaceutical Solid Dosage Forms* Lubricants, 2014. **2**: p. 21-43.
71. Morin, G. and L. Briens, *The Effect of Lubricants on Powder Flowability for Pharmaceutical Application.* AAPS PharmSciTech, 2013. **14**(3): p. 1158-1168.
72. D. Brone, A.A., and F.J. Muzzio, *Quantitative Characterization of Mixing of Dry Powders in V-blenders.* AIChE Journal, 1998. **44**(2): p. 271-278.
73. (Pfizer), S.B. *Solid Oral Dosage Forms Powder Blending*. in *IKEV Meeting*. 2001. Cork, Ireland.
74. Pharmacopeia, U.S., *<616> Bulk Density and Tapped Density of Powders* 2012.
75. Bruno C. Hancock, J.T.C., Matthew P. Mullarney, Andrey V. Zinchuk, *The Relative Densities of Pharmaceutical Powders, Blends, Dry Granulations, and Immediate-Release Tablets.* Pharmaceutical Technology, 2003, April: p. 64-80.
76. Pharma, D., *Lactose - Some basic properties and characteristics*.
77. Sun, C.C., *True Density of Microcrystalline Cellulose.* Journal of Pharmaceutical Sciences, 2005, October. **94**(10): p. 2132-2134.
78. U. I. Leinonen, H.U.J., P. A. Vihervaara, E. S. U. Laine, *Physical and Lubrication Properties of Magnesium Stearate.* Journal of Pharmaceutical Sciences, 1992, December. **81**(12): p. 1194-1198.
79. Singh, R., M. Ierapetritou, and R. Ramachandran, *An engineering study on the enhanced control and operation of continuous manufacturing of pharmaceutical tablets via roller compaction.* International Journal of Pharmaceutics, 2012. **438**(1–2): p. 307-326.

NOMENCLATURE

Abbreviations

WHO	World Health Organization
R&D	Research and Development
NME	New Molecular Entity
NDA	New Drug Application
FDA	Food and Drug Administration
PAT	Process Analytical Techniques
QbD	Quality by Design
QC	Quality Control
QA	Quality Assurance
PSE	Process System Engineering
DEM	Discrete Element Modeling
FEM	Finite Element Modeling
CFD	Computational Fluid Dynamics
PBM	Population Balance Modeling
RTD	Residence Time Distribution
ROM	Reduced Order Models
API	Active Pharmaceutical Ingredient
DC	Direct Compaction
WG	Wet Granulation
DG	Dry Granulation
MCC	Microcrystalline cellulose
APAP	Acetaminophen
USP	United States Pharmacopeia
PCA	Principal Component Analysis
PC1	Principal Component 1
PC2	Principal Component 2
MCF	Main compression force
PCF	Pre-compression force
MgSt	Magnesium Stearate
RMSE	Root Mean Square Error

Symbols

D	Relative density
D_0	Initial relative density
P	Compression pressure
k	Proportionality constant
ε	Porosity
A, B, m, a	Parameters

ε_0	Initial porosity
ρ_{true}	True density
b	Kawakita parameter
C	Relative change in volume
V_i	Initial volume
V_f	Final volume
H_{tablet}	Tablet hardness
$H_{\max}$	Maximum hardness
ρ_r	Relative density
ρ_{rc}	Critical relative density
λ_{hard}	Function of relative density and critical relative density
V_{solid}	Volume of solid fraction
V_{tablet}	Volume of tablet
ρ_{bulk}	Bulk density
ρ_{tapped}	Tapped Density
m	Mass
V_0	Initial volume
V_t	Volume after tapping
H	Haunser ratio
CI	Carr Index
ΔP	Pressure drop
q	Air flow rate
η	Viscosity of air
L	Height of the powder bed
κ	Permeability
σ	Cohesion
ρ_{true}^{mix}	True density of a mixture
ρ_{true}^{i}	True density of a pure component
w_A	Mass of component ‘A’ in the mixture
w_B	Mass of component ‘B’ in the mixture
ΔV	Percent volume change (Compressibility)

Superscripts

mix	Mixture
i	Pure component ‘i’

Subscripts

0	Initial
$true$	True or Absolute

f	Final
$tablet$	Of tablet
$\max$	Maximum
r	Relative
rc	Critical relative
λ_{hard}	Function of relative density and critical relative density
$solid$	Solid fraction
$bulk$	Bulk or whole
$tapped$	After tapping
A	Component ‘A’
B	Component ‘B’

APPENDIX 1

Parity plots for main compression force to compare the fit between model output and experimental data for all the blends.

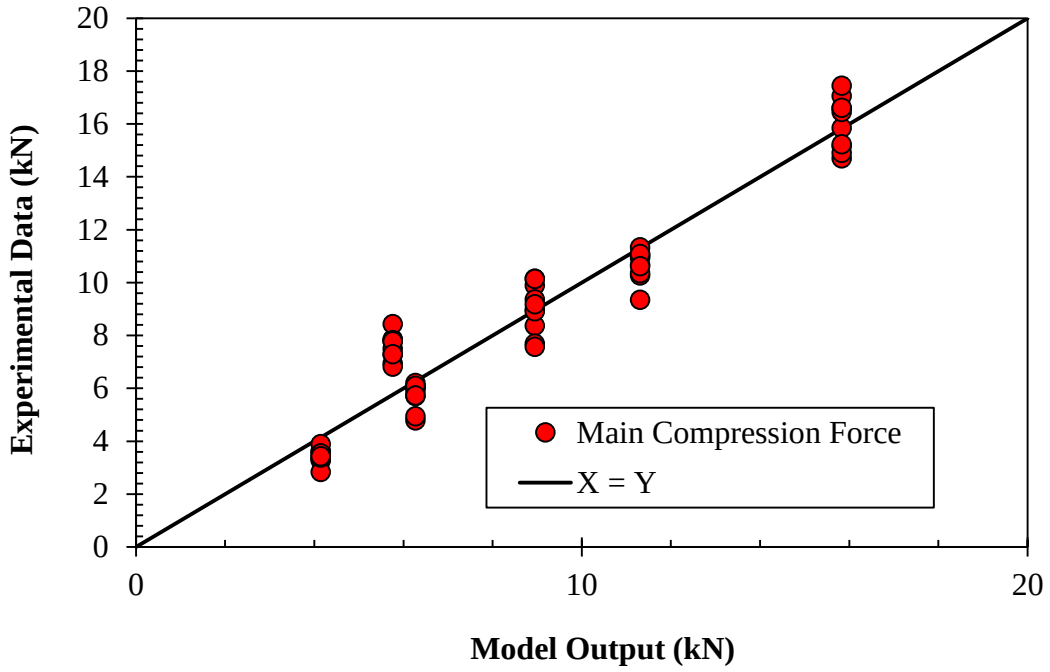

Figure 24. Parity plot for main compression of lactose with 0.25% magnesium stearate.

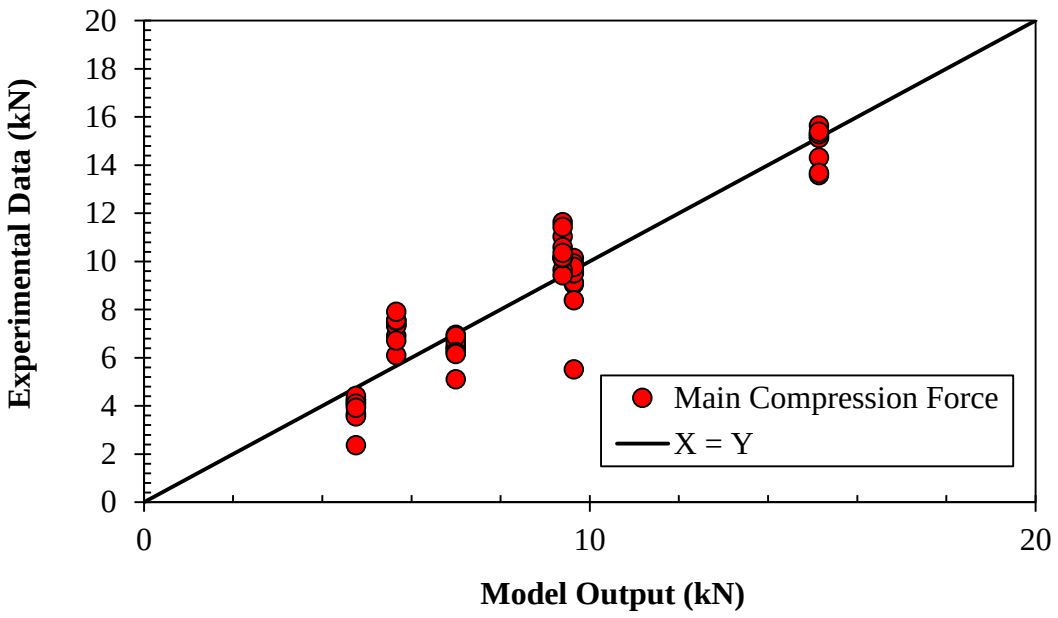

Figure 25. Parity plot for main compression of lactose with 0.75% magnesium stearate.

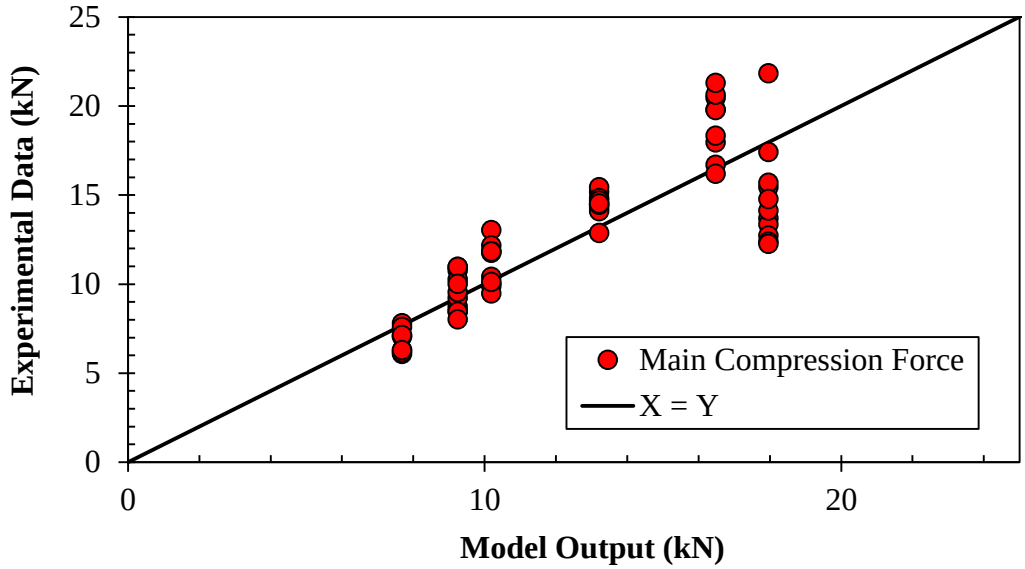

Figure 26. Parity plot for main compression of lactose with 1% magnesium stearate.

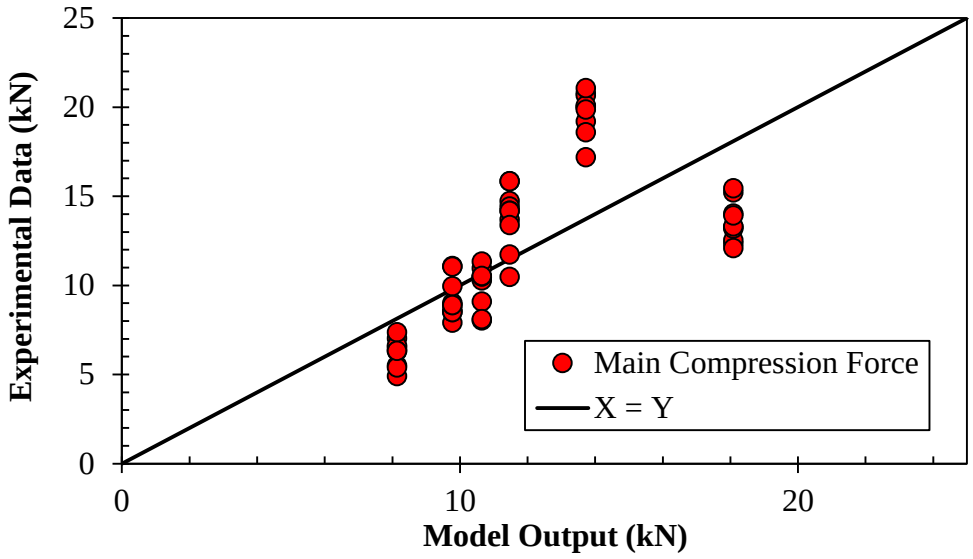

Figure 27. Parity plot for main compression of lactose with 1.5% magnesium stearate.

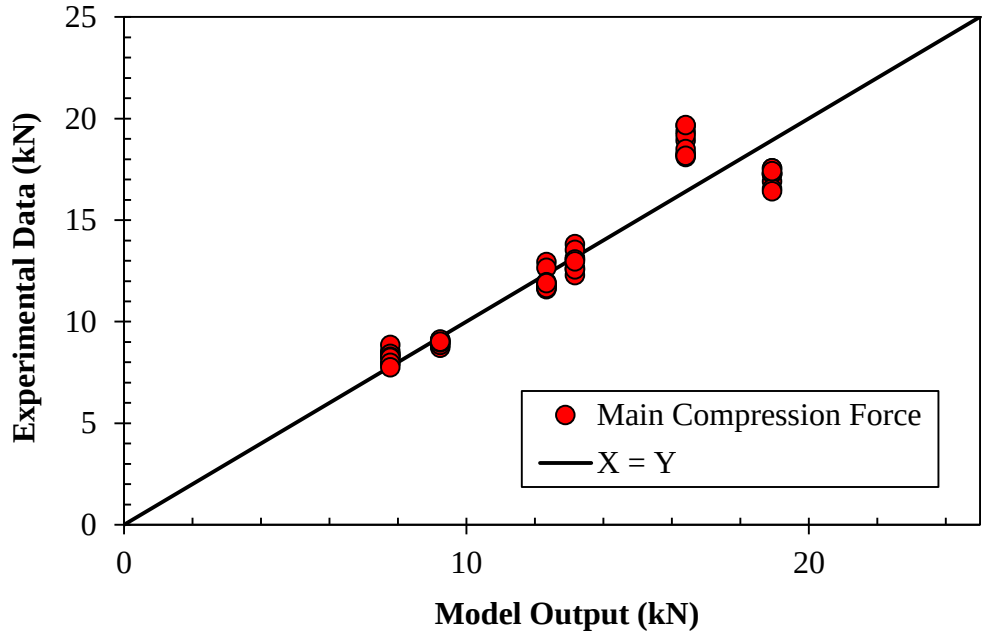

Figure 28. Parity plot for main compression of Avicel 101 with 0.25% magnesium stearate.

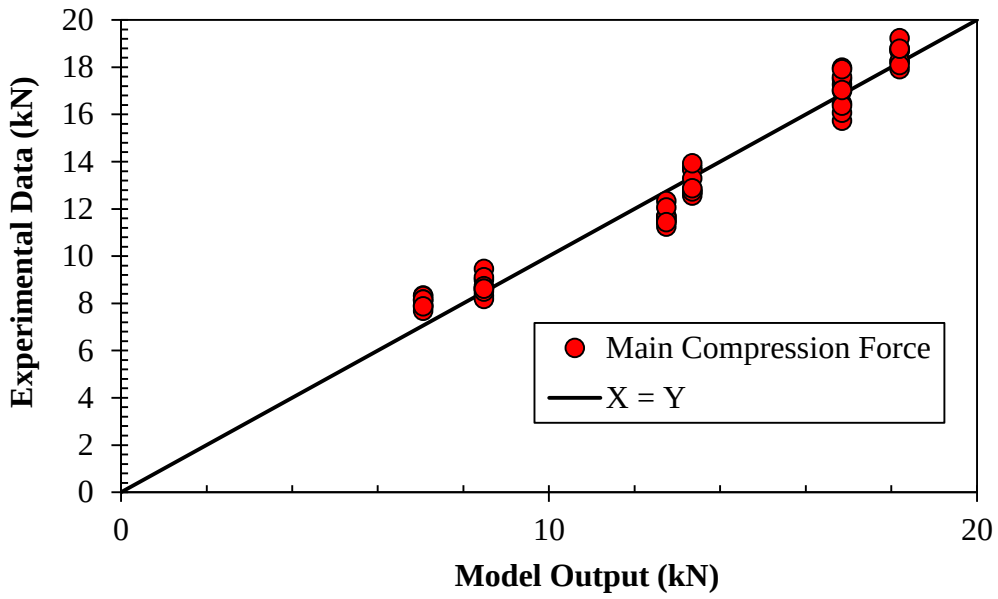

Figure 29. Parity plot for main compression of Avicel 101 with 0.75% magnesium stearate.

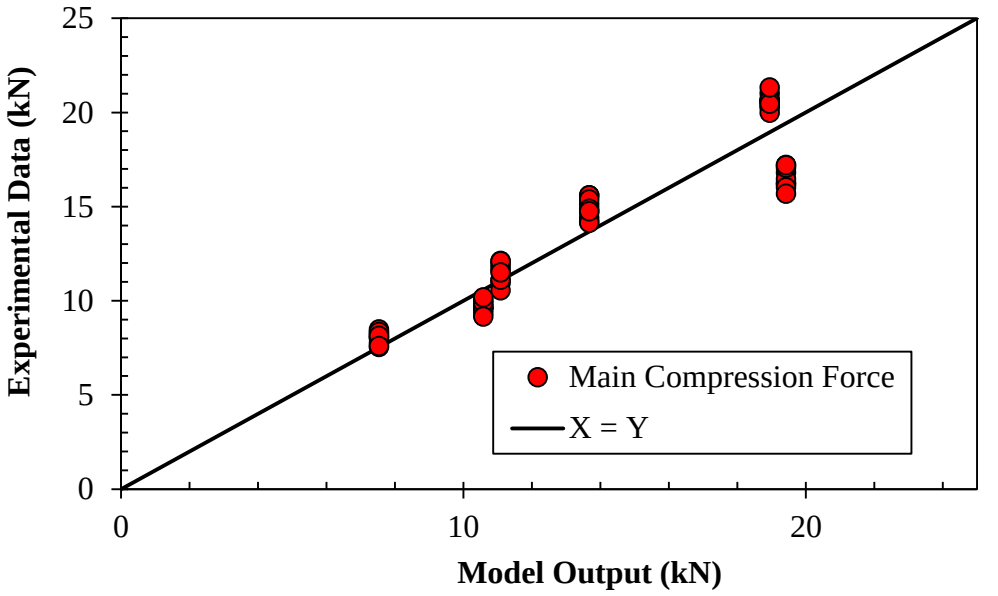

Figure 30. Parity plot for main compression of Avicel 101 with 1% magnesium stearate.

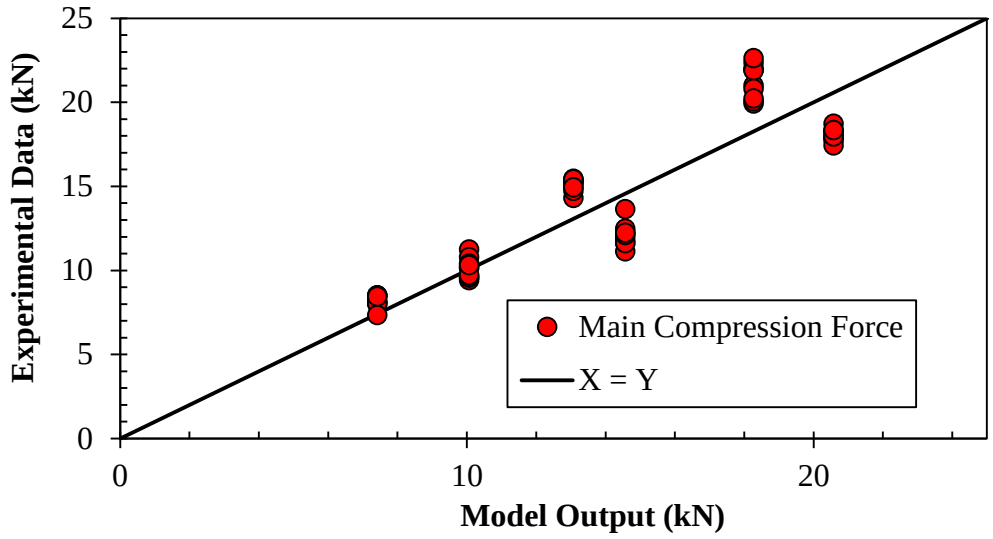

Figure 31. Parity plot for main compression of Avicel 101 with 1.5% magnesium stearate.

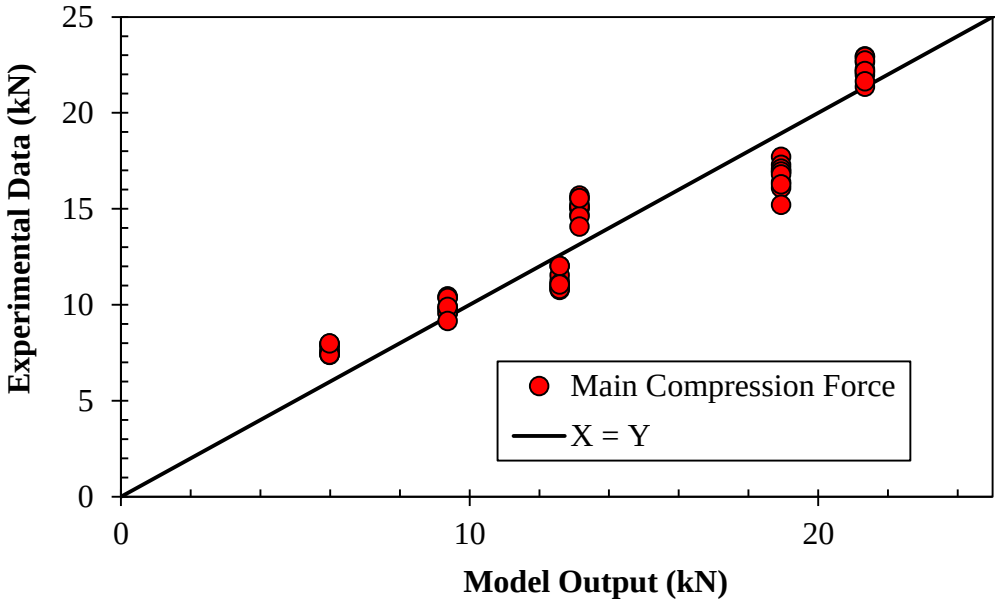

Figure 32. Parity plot for main compression of Avicel 301 with 0.25% magnesium stearate.

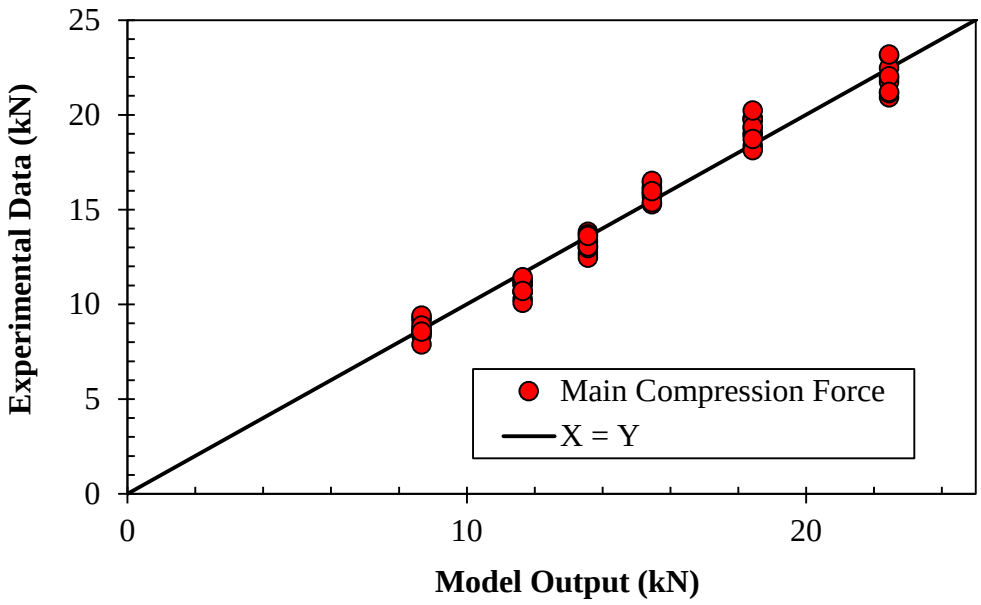

Figure 33. Parity plot for main compression of Avicel 301 with 0.75% magnesium stearate.

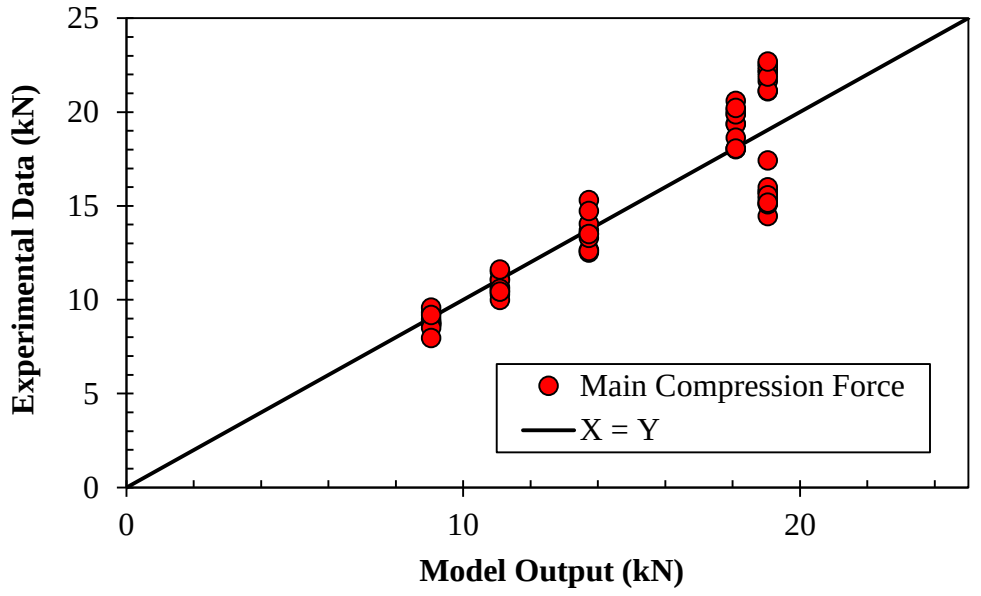

Figure 34. Parity plot for main compression of Avicel 301 with 1% magnesium stearate.

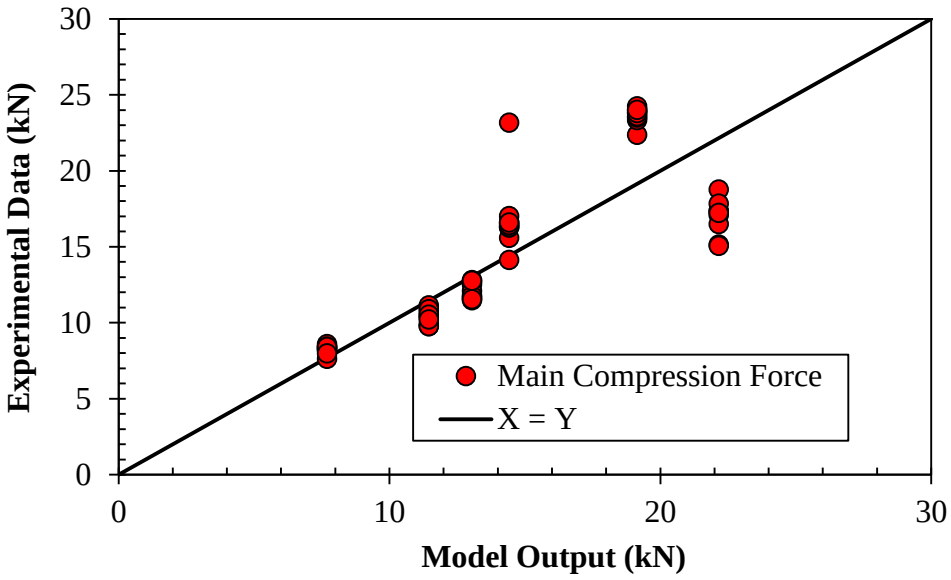

Figure 35. Parity plot for main compression of Avicel 301 with 1.5% magnesium stearate.

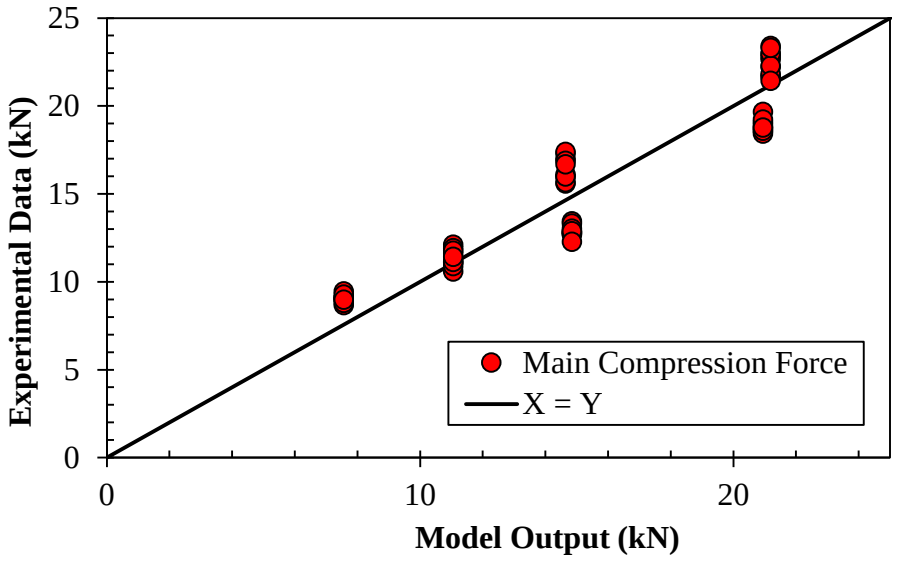

Figure 36. Parity plot for main compression of APAP and Avicel 101 with 0.25% magnesium stearate.

APPENDIX 2

Compression parameters applied (i.e. fill depth, pre-compression length and tablet thickness) for all the blends have been tabulated below.

Table 15. Compression parameters for lactose with 0.25% magnesium stearate.

Condition	Dosing Position or Fill Depth (mm)	Pre-compression Position (mm)	Compression Position or Tablet Thickness (mm)
1	5.75	4	2.75
2	5.75	4	2.5
3	5.75	4	2.25
4	5	4	2.75
5	5	4	2.5
6	5	4	2.25

Table 16. Compression parameters for lactose with 0.75% magnesium stearate.

Condition	Dosing Position or Fill Depth (mm)	Pre-compression Position (mm)	Compression Position or Tablet Thickness (mm)
1	5.75	4	2.75
2	5.75	4	2.5
3	5.75	4	2.25
4	5	4	2.75
5	5	4	2.5
6	5	4	2.25

Table 17. Compression parameters for lactose with 1% magnesium stearate.

Condition	Dosing Position or Fill Depth (mm)	Pre-compression Position (mm)	Compression Position or Tablet Thickness (mm)
1	5.75	4	2.5
2	5.75	4	2.25
3	5.75	4	2
4	5.25	4	2.5
5	5.25	4	2.25
6	5.25	4	2

Table 18. Compression parameters for lactose with 1.5% magnesium stearate.

Condition	Dosing Position or Fill Depth (mm)	Pre-compression Position (mm)	Compression Position or Tablet Thickness (mm)
1	5.75	4	2.5
2	5.75	4	2.25
3	5.75	4	2
4	5.25	4	2.5
5	5.25	4	2.25
6	5.25	4	2

Table 19. Compression parameters for Avicel 101 with 0.25% magnesium stearate.

Condition	Dosing Position or Fill Depth (mm)	Pre-compression Position (mm)	Compression Position or Tablet Thickness (mm)
1	10.75	5	2.25
2	10.75	5	2
3	10.75	5	1.75
4	10.25	5	2.25
5	10.25	5	2
6	10.25	5	1.75

Table 20. Compression parameters for Avicel 101 with 0.75% magnesium stearate.

Condition	Dosing Position or Fill Depth (mm)	Pre-compression Position (mm)	Compression Position or Tablet Thickness (mm)
1	10.75	5	2.25
2	10.75	5	2
3	10.75	5	1.75
4	10.25	5	2.25
5	10.25	5	2
6	10.25	5	1.75

Table 21. Compression parameters for Avicel 101 with 1% magnesium stearate.

Condition	Dosing Position or Fill Depth (mm)	Pre-compression Position (mm)	Compression Position or Tablet Thickness (mm)
1	10.75	5	2.25
2	10.75	5	2
3	10.75	5	1.75
4	10.25	5	2.25
5	10.25	5	2
6	10.25	5	1.75

Table 22. Compression parameters for Avicel 101 with 1.5% magnesium stearate.

Condition	Dosing Position or Fill Depth (mm)	Pre-compression Position (mm)	Compression Position or Tablet Thickness (mm)
1	10.75	5	2.25
2	10.75	5	2
3	10.75	5	1.75
4	10.25	5	2.25
5	10.25	5	2
6	10.25	5	1.75

Table 23. Compression parameters for Avicel 301 with 0.25% magnesium stearate.

Condition	Dosing Position or Fill Depth (mm)	Pre-compression Position (mm)	Compression Position or Tablet Thickness (mm)
1	8.5	5	1.75
2	8.5	5	2
3	8.5	5	2.25
4	8	5	1.75
5	8	5	2
6	8	5	2.25

Table 24. Compression parameters for Avicel 301 with 0.75% magnesium stearate.

Condition	Dosing Position or Fill Depth (mm)	Pre-compression Position (mm)	Compression Position or Tablet Thickness (mm)
1	8.5	5	1.75
2	8.5	5	2
3	8.5	5	2.25
4	8	5	1.75
5	8	5	2
6	8	5	2.25

Table 25. Compression parameters for Avicel 301 with 1% magnesium stearate.

Condition	Dosing Position or Fill Depth (mm)	Pre-compression Position (mm)	Compression Position or Tablet Thickness (mm)
1	8.5	5	1.75
2	8.5	5	2
3	8.5	5	2.25
4	8	5	1.75
5	8	5	2
6	8	5	2.25

Table 26. Compression parameters for Avicel 301 with 1.5% magnesium stearate.

Condition	Dosing Position or Fill Depth (mm)	Pre-compression Position (mm)	Compression Position or Tablet Thickness (mm)
1	8.5	5	1.75
2	8.5	5	2
3	8.5	5	2.25
4	8	5	1.75
5	8	5	2
6	8	5	2.25

Table 27. Compression parameters for APAP (15%) + Avicel 301 with 1% magnesium stearate.

Condition	Dosing Position or Fill Depth (mm)	Pre-compression Position (mm)	Compression Position or Tablet Thickness (mm)
1	10	5	1.75
2	10	5	2
3	10	5	2.25
4	9.5	5	1.75
5	9.5	5	2
6	9.5	5	2.25

APPENDIX 3

Comparison between the model predicted and regressed parameter values have been tabulated below.

Table 28. Comparison between calculated and regressed compression parameters.

Blend	Pre-compression Parameter (MPa^{-1})		Percent Difference	Main Compression Parameter (MPa^{-1})		Percent Difference
	Predicted	Regressed	(%)	Predicted	Regressed	(%)
1	0.0583	0.0555	4.95%	0.0423	0.0412	2.76%
2	0.0468	0.0519	-9.88%	0.0385	0.0322	19.41%
3	0.0586	0.0602	-2.70%	0.0256	0.0264	-2.79%
4	0.0511	0.0526	-2.91%	0.0225	0.0237	-5.42%
5	0.1498	0.1446	3.61%	0.0291	0.0278	4.53%
6	0.1451	0.1512	-4.02%	0.0329	0.0373	-11.94%
7	0.1493	0.1529	-2.39%	0.0421	0.0382	10.12%
8	0.1527	0.1581	-3.43%	0.0326	0.0398	-18.12%
9	0.1210	0.1247	-2.92%	0.0484	0.0563	-14.03%
10	0.1222	0.1178	3.72%	0.0376	0.0382	-1.68%
11	0.1307	0.1219	7.21%	0.0396	0.0343	15.68%
12	0.1150	0.1165	-1.23%	0.0372	0.0318	17.12%
13	0.1338	0.1457	-8.18%	0.0521	0.0389	33.68%

Table 29. Comparison between calculated and regressed hardness parameter.

Blend	Maximum Hardness (MPa)		Percent Difference
	Predicted	Regressed	(%)
1	4.5132	4.4620	1.15%
2	4.2914	4.3120	-0.48%
3	4.6099	4.5300	1.76%
4	4.2512	4.2600	-0.21%
5	16.9349	16.7270	1.24%
6	14.8468	15.1880	-2.25%
7	16.6414	17.0000	-2.11%
8	12.7444	12.5950	1.19%
9	12.1679	12.1100	0.48%
10	10.0684	10.3360	-2.59%
11	10.6054	9.3540	13.38%
12	8.8688	8.7050	1.88%
13	13.2684	10.5410	25.87%

Table 30. Comparison between calculated and regressed critical relative density.

Blend	Critical Relative Density (-)		Percent Difference
	Predicted	Regressed	(%)
1	0.7868	0.7990	-1.53%
2	0.8143	0.8075	0.84%
3	0.8385	0.8466	-0.95%
4	0.8488	0.8439	0.58%
5	0.6375	0.6220	2.49%
6	0.6420	0.6557	-2.10%
7	0.6572	0.6264	4.93%
8	0.6654	0.6200	7.32%
9	0.6661	0.7028	-5.22%
10	0.6782	0.6823	-0.61%
11	0.7011	0.6722	4.29%
12	0.6678	0.6590	1.34%
13	0.6260	0.6459	-3.08%

APPENDIX 4

Detailed statistical analysis result tables have been included below.

Table 31. Results of PCA.

Eigen analysis of the Correlation Matrix									
Eigenvalue	6.3168	1.5415	0.7205	0.2901	0.0776	0.0506	0.0023	0.0005	0.0001
Proportion	0.702	0.171	0.080	0.032	0.009	0.006	0.000	0.000	0.000
Cumulative	0.702	0.873	0.953	0.985	0.994	1.000	1.000	1.000	1.000
Variable	**PC1**	**PC2**	**PC3**	**PC4**	**PC5**	**PC6**	**PC7**	**PC8**	**PC9**
Bulk Density	-0.365	-0.214	0.138	-0.472	-0.308	-0.042	-0.351	-0.595	0.065
Tapped Density	-0.363	-0.242	0.158	-0.427	-0.257	-0.121	0.237	0.678	-0.082
Cohesion	0.184	-0.393	-0.857	-0.254	0.048	-0.087	0.050	-0.017	-0.006
Pressure Drop	-0.358	-0.317	0.046	0.017	0.428	0.649	0.371	-0.160	-0.037
Compressi-bility	-0.209	-0.614	0.036	0.684	-0.216	-0.220	-0.122	0.013	0.000
Mean Particle Size	0.365	-0.267	0.242	-0.126	0.122	0.006	-0.150	-0.037	-0.826
D10	0.387	-0.054	0.031	0.045	-0.723	0.439	0.343	-0.103	0.030
D50	0.345	-0.300	0.348	-0.162	0.222	-0.441	0.488	-0.231	0.328
D90	0.357	-0.317	0.193	-0.131	0.144	0.344	-0.535	0.308	0.444

Table 32. PLS regression results for pre-compression and main compression Kawakita parameter.

Method	
Cross-validation	Leave-one-out
Components to evaluate	Set
Number of components evaluated	7
Number of components selected	4

Predictor Variables	**Pre-compression Kawakita parameter**		**Main compression Kawakita parameter**	
	Coefficient	**Standardized coefficient**	**Coefficient**	**Standardized coefficient**
Constant	0.243530	0.000000	0.093370	0.000000
Bulk Density	-0.172368	-0.527613	0.033880	0.444962
Tapped Density	-0.118930	-0.535043	0.023321	0.450157
Cohesion	-0.019816	-0.080852	-0.018494	-0.323765
Pressure Drop	-0.001147	-0.110708	-0.000749	-0.310261
Compressibility	0.005145	0.128636	-0.007852	-0.842381
Mean PS	-0.000102	-0.019847	0.000166	0.139272
D10	-0.000160	-0.016140	0.000573	0.247968
D50	-0.000280	-0.045150	0.000250	0.172959
D90	-0.000080	-0.028222	0.000061	0.092599

Table 33. PLS regression results for maximum hardness.

Method	
Cross-validation	Leave-one-out
Components to evaluate	Set
Number of components evaluated	7
Number of components selected	5

Predictor Variables	**Maximum Hardness**	
	Coefficient	**Standardized coefficient**
Constant	12.257000	0.000000
Bulk Density	-16.873500	-0.487614
Tapped Density	-11.164600	-0.467043
Cohesion	-4.710600	-0.150285
Pressure Drop	0.250800	0.217283
Compressibility	0.163100	0.033006
Mean PS	0.075700	0.115940
D10	0.176300	0.157400
D50	-0.085400	-0.104728
D90	0.093100	0.263177

Table 34. PLS regression results for critical relative density.

Method	
Cross-validation	Leave-one-out
Components to evaluate	Set
Number of components evaluated	7
Number of components selected	2

Predictor Variables	**Critical Relative Density**	
	Coefficient	**Standardized coefficient**
Constant	0.289843	0.000000
Bulk Density	0.154691	0.245990
Tapped Density	0.109135	0.251222
Cohesion	-0.062008	-0.108859
Pressure Drop	0.004627	0.220550
Compressibility	0.020099	0.223745
Mean PS	-0.000129	-0.010883
D10	-0.001741	-0.085514
D50	0.000226	0.015280
D90	0.000043	0.006619

APPENDIX 5

Tablet Press Model Equations

The tablet press model has been briefly described in this section. The model details can be found in Singh et al. (2010, 2012) [66, 79].

Tablet geometry: Flat cylinder

1. Area of tablet:

$$A_{tablet} = \frac{\pi\,(d_{tablet})^2}{4}$$

2. Since, the shape of the tablet is that of a cylinder, volume of tablet is calculated using geometrical equation for a cylinder.

$$V_{tablet} = L_{tablet}\ A_{tablet}$$

3. The feed volume for the tablet is associated to the fill depth or the position of the lower punch in the die during the initial filling stage.

$$V_0 = L_{depth}\ A_{tablet}$$

4. The following equation gives the pre-compression volume of the tablet. It uses the pre-compression length, which is the height of the powder in the die after the pre-compression stage and is input into the model.

$$V_{pre} = L_{pre}\ A_{tablet}$$

5. The weight of the tablet is calculated based on the bulk density and feed volume of the powder in the die.

$$M_{tablet} = V_0\ \rho_{bulk}$$

6. The pre-compression and main compression forces are calculated via the Kawakita compression equations. These equations give the peak compression force and use a material dependent parameter, b, known as the Kawakita parameter.

$$\lambda_{pre} = V_0\ (\varepsilon_0 - 1) + V_{pre}$$

   If the true density of the powder blend is known, the initial porosity can be computed using the relation between bulk and true density.

$$\rho_{true} = \rho_{bulk}(1-\varepsilon_0)$$

$$CP_{pre} = \frac{(V_0 - V_{pre})}{b_{pre}\lambda_{pre}}$$

7. The pre-compression force equation involves multiplication with 10^6 to adjust the units of force.

$$CF_{pre} = 10^6\ CP_{pre}\ A_{tablet}$$

8. The change in porosity of the tablet after pre-compression is recalculated and termed as main porosity or porosity before main compression in the model.

$$\varepsilon_{main} = 1-((1-\varepsilon_0)\,V_0/V_{pre})$$

$$\lambda_{main} = V_{pre}\ (\varepsilon_{main} - 1) + V_{tablet}$$

$$CP_{main} = \frac{(V_{pre} - V_{tablet})}{b_{main}\lambda_{main}}$$

9. Again, the multiplication with 10^6 is to adjust the units of force.

$$CF_{main} = 10^6\ CP_{main}\ A_{tablet}$$

10. The solid volume of the powder is calculated based on porosity and feed volume.

$$V_{solid} = (1-\varepsilon_0)\,V_0$$

11. Relative density is necessary to obtain the hardness of the tablet via Kuentz hardness model.

$$\rho_r = \frac{V_{solid}}{V_{tablet}}$$

$$\lambda_{hard} = \log(\frac{1-\rho_r}{1-\rho_{rc}})$$

12. Tablet hardness is to be optimized for a given weight of tablet and is given by the following equation. It uses maximum hardness, which is defined as the hardness at zero porosity.

$$H_{tablet} = H_{\max}\,(1-e^{(\rho_r - \rho_{rc} + \lambda_{hard})})$$

13. The rate of tablet production set point is calculated from the flow rate coming in using fundamental mass balance and the turret speed set point is subsequently calculated from the rate of tablet production set point.

$$F_{in} = R_{set}\ M_{tablet}$$

$$R_{set} = T_{set}\ N_{die}\ 60$$

14. The turret speed has been modelled as a first order response,

$$\tau \frac{dT_{speed}(t)}{dt} + T_{speed}(t) = T_{set}$$

So is the fill depth, tablet thickness, pre-compression and main compression forces.

15. The actual rate of tablet production depends on the variation in the turret speed and can be given by the equation,

$$R_{tablet}(t) = T_{speed}(t)\ N_{die}\ 60$$

16. Mass flow rate out of the tablet press is predicted as given below.

$$F_{out}(t) = R_{tablet}(t)\ M_{tablet}$$